

VILNIUS UNIVERSITY

KRISTINA KLEMKAITĖ-RAMANAUSKĖ

SYNTHESIS, MODIFICATION AND CHARACTERIZATION OF Mg/Al,
Co/Mg/Al AND Ni/Mg/Al LAYERED DOUBLE HYDROXIDES

Doctoral Dissertation

Physical Sciences, Chemistry (03P)

Vilnius, 2012

The dissertation was carried out at the Vilnius University in the period of 2007-2012.

Scientific supervisors:

Prof. Habil. Dr. Aivaras Kareiva (Vilnius University, Physical Sciences, Chemistry 03P) (2007-2009);

Prof. Dr. Aldona Beganskienė (Vilnius University, Physical Sciences, Chemistry 03P) (2009-2011).

Scientific consultant:

Dr. Alexander Khinsky (Amiagus, Nortá Ltd.).

ACKNOWLEDGEMENTS

I would like to express my utmost gratitude to my supervisors Prof. Aivaras Kareiva and Dr. Alexander Khinsky. The support, freedom and trust provided by the Prof. Aivaras Kareiva are greatly acknowledged. I feel honored for working many years with Dr. Alexander Khinsky and very thankful for guiding me through the field of layered double hydroxides applications. I also would like to thank Prof. Dr. Aldona Beganskienė for agreeing to be my supervisor last years of my PhD. I sincerely appreciate the help and support provided by Rimantas Pakamanis, president of Ltd. Norta, without whom my research, most probably, would have not even been started. I am very happy for getting this topic for my PhD thesis and I hope that works with LDH will continue in the Vilnius University.

I would kindly like to thank Prof. Antonio Eduardo Palomares Gimeno and Prof. Avelino Corma Canos (Polytechnic University of Valencia) for helping me with investigations of morphology and catalytic activity in NO_x removal of cobalt containing layered double hydroxides. I appreciate the patience of Prof. A.E. Palomares during our discussions and spent time trying to help me finding answers for arising questions.

I would also wish to thank Prof. Francesco Basile and Patricia Benito (University of Bologna) for a nice time and interesting discussions about layered double hydroxides and their applications in catalysis during my several visits to Bologna.

I would like to acknowledge many people for providing important experimental measurements: Arūnas Baltušnikas (Kaunas University of Technology) - XRD, Kęstutis Baltakys (Kaunas University of Technology) - thermal analysis, Ričardas Taraškevičius (Institute of Geology and Geography) -

XRF, Algirdas Selskis (Center for Physical Sciences and Technology) - SEM and Jiří Pinkas (Masaryk University) - BET/BJH.

I am also indebted to Ieva Balčiūnaitė, Erika Čiužauskienė, Paulius Lučinskas, Vitas Pakamanis, Kazys Babilius and to many other colleagues from Norta Ltd. for very nice working environment and especially to Nerijus Laurinaitis for assistance with the experiments.

I appreciate all of my friends and colleagues who provided a nice atmosphere in the Vilnius University during the time of my PhD studies. My thanks for a nice time and interesting discussions during the coffee breaks go to the: Albinas Žilinskas, Darius Jasaitis, Audronė Jankevičiūtė, Olga Darčanova, Simas Šakirzanovas, Jurgis Pilipavičius, Danas Sakalauskas, Irma Bogdanovičienė and many others. Teresa Subatniekienė and Rimantas Raudonis are also greatly acknowledged for their help with administration tasks during the studies at Vilnius University.

I would also like to thank my good friends for being with me during all these years and helping me to have a wonderful time while I am not working: Agnė, Laura, Renata, Gražina, Gintarė, Karolina, Nerijus, Aleksandras and others. I am very happy for having a very good friend Linas Vilčiauskas who was always helping me when I needed advises not only in chemistry topics. I certainly learned a lot from him. Thanks to all of my friends from all over the world Audronė, Dodo, Sanjay, Angel, Jonathan and many others with whom I had wonderful time during my trips.

I want to thank my chemistry teacher Genovaitė Banevičienė, for introducing me the world of chemistry.

Most importantly, I'd like to thank my family for their continual support and belief in my success. This thesis would have not been written without the help of my husband, mother, brother, aunt, mother in law and, of course my little daughter, who has even prolonged the great time off my PhD.

TABLE OF CONTENTS

| | |
|---|-----------|
| INTRODUCTION | 8 |
| 1. LITERATURE SURVEY | 12 |
| 1.1. LAYERED DOUBLE HYDROXIDES | 12 |
| 1.1.1. Cations in LDH | 14 |
| 1.1.2. Anions in LDH | 14 |
| 1.2. SYNTHESIS METHODS OF LDH | 15 |
| 1.2.1. Direct methods | 15 |
| 1.2.2. Indirect methods | 18 |
| 1.3. PROPERTIES AND APPLICATION OF LDH | 21 |
| 1.3.1. Properties of Mg/Al layered double hydroxide | 21 |
| 1.3.2. Application of Mg/Al LDH | 26 |
| 1.3.3. Properties of Co/Mg/Al layered double hydroxide | 27 |
| 1.3.4. Application of Co/Mg/Al LDH | 29 |
| 1.3.5. Properties of Ni/Mg/Al layered double hydroxide | 30 |
| 1.3.6. Application of Ni/Mg/Al LDH | 32 |
| 2. EXPERIMENTAL | 33 |
| 2.1. MATERIALS | 33 |
| 2.2. SYNTHESIS AND POST-SYNTHESIS MODIFICATIONS | 34 |
| 2.2.1. Mg/Al LDH | 34 |
| 2.2.2. Co/Mg/Al LDH and Ni/Mg/Al LDH | 34 |
| 2.3. CHARACTERIZATION | 36 |
| 2.4. ACTIVITY STUDIES | 38 |
| 3. RESULTS AND DISCUSSIONS | 40 |
| 3.1. SYNTHESIS OF LDHs BY COPRECIPITATION METHOD AND X-RAY CHARACTERISATION | 40 |

| | | |
|-----------|---|-----------|
| 3.2. | THERMAL DECOMPOSITION OF LDH | 44 |
| 3.3. | REFORMATION OF LDH IN WATER | 48 |
| 3.4. | REFORMATION OF LDH IN $Mg(NO_3)_2$ SOLUTION | 54 |
| 3.5. | INFLUENCE OF REFORMATION ON MORPHOLOGY | 59 |
| 3.6. | APPLICATION OF REFORMED LDH | 66 |
| 4. | CONCLUSIONS | 73 |
| | REFERENCES | 75 |
| | LIST OF PUBLICATIONS | 85 |
| | CURRICULUM VITAE | 87 |
| | SUMMARY IN LITHUANIAN (SANTRAUKA) | 88 |

GLOSSARY

^{27}Al MAS NMR – ^{27}Al Magic Angle Spinning Nuclear Magnetic Resonance

BET – Brunauer Emmet Teller

BJH – Barret Joyner Halenda

DSC - Differential Scanning Calorimetry

DTA - Differential Thermal Analysis

DTG - Differential Thermogravimetry

EDXRD - Energy-Dispersive X-ray Diffraction

EVA – Ethylene Vinyl Acetate

FTIR - Fourier Transform Infrared

FWHM - Full Width at Half Maximum

HT - Hydrotalcite

HTC - Hydrotalcite-Type Compounds

IFD - Interlayer Free Distance

LDH - Layered Double Hydroxides

NSR - NO_x Storage/Reduction

NTP - Normal Temperature and Pressure

ppm - Parts per million

PVC – Polyvinyl Chloride

SEM - Scanning Electron Microscope

STA - Simultaneous Thermal Analysis

TG – Thermogravimetry

TPR - Temperature-Programmed Reduction

VOC - Volatile Organic Compounds

XAFS - X-ray Absorption Fine Structure

XRD – X-ray Diffraction

XRF – X-ray Fluorescence

INTRODUCTION

The background for this doctoral thesis stems from the need to investigate the properties of synthesized, decomposed and reconstructed layered double hydroxides (LDH), with the aim to understand and control the composition and structure of the LDHs and derived oxides. Layered double hydroxides, hydrotalcite-type compounds (HTC) or anionic clays are the commonly used names to describe a class of layered materials based on the brucite ($\text{Mg}(\text{OH})_2$) crystal structure and having a general chemical formula of $[\text{M}^{\text{II}}_{1-x} \text{M}^{\text{III}}_x(\text{OH})_2]^{x+}(\text{A}^{\text{m-}})_{x/m} \cdot n\text{H}_2\text{O}$ [1-3]. The structure of LDHs is comprised of positively charged metal hydroxide layers $[\text{M}^{\text{II}}_{1-x} \text{M}^{\text{III}}_x(\text{OH})_2]^{x+}$ and negatively charged anions $(\text{A}^{\text{m-}})_{x/m}$ in the interlayer space. The molecules of H_2O are usually present in the interlayer space. A large number of LDHs can be synthesized by varying either the type of the cation or anion resulting in numerous new materials showing specific properties. For example, the optimization of catalytic processes very often requires the substitution of liquid acids and bases by more environmentally friendly solid catalysts. For this case, anionic clays may be considered a very promising alternative. Their high versatility, easily controllable properties, wide range of preparation routes, low cost etc. make them of extreme interest in various applications. LDHs are used as ion-exchangers, adsorbents [4-9], catalysts [2, 10-12], and others [3].

Although LDHs have different chemical compositions they share typical common characteristics: layered structure and the formation of mixed-metal oxides after thermal treatment. Layered double hydroxides can be prepared with different divalent and trivalent cations in the structure serving as precursors for the preparation of mixed metal oxides used as catalysts for oxidation and hydrogenation/dehydrogenation reactions. The exact features, such as the nature of the cations in the brucite-like layers and the specific surface area may have a

significant effect on their final catalytic properties. The synthesis of high surface area LDHs, derived mixed oxides and their ability to reconstitute are very interesting, since they should affect the active sites of the solid as well as its catalytic activity. In this work, the LDH containing Mg and Al cations which is identical to the natural hydrotalcite was mostly used as a reference system. LDH containing nickel or cobalt transition metals were synthesized and investigated using various techniques. Cobalt containing hydrotalcites are interesting as the basis for the preparation of the active catalyst for NO removal in automotive applications [13, 14]. Nickel containing LDH was selected as a basis for gasification, catalytic partial oxidation or steam reforming applications [15-18].

The simplest method to obtain modified LDH is to replace the cations in the brucite-type layer with others which have a similar ionic radius to Mg^{2+} or Al^{3+} and can adopt the same octahedral arrangement. Metals which are not compatible with the octahedral sites of the brucite-type sheet may be introduced in the interlayer space of these solids in their anionic form. In this thesis, the synthesis of Mg/Al, Co/Mg/Al and Ni/Mg/Al LDHs using co-precipitation at low supersaturation method was chosen as a direct method to prepare materials. Afterwards, the synthesized LDHs were thermally decomposed followed by the indirect method, reformation, to get the LDHs again. Investigation of mixed oxides derived from calcined direct and indirect synthesized LDHs is an interesting topic, since the reformation media could have an effect not only on the composition of a solid but also on the morphology of oxides. The surface area and the total number of active sites are important quantities for the catalytic activity of these materials. The possibility to control and improve these characteristics is one of the central themes of this study.

The main aims of the study

The objectives of this study are to prepare three types of LDHs with selected composition using the co-precipitation method and to investigate their properties as obtained, after decomposition and reformation. The following tasks were set in order to achieve these objectives:

- Synthesis of Mg/Al, Co/Mg/Al and Ni/Mg/Al LDHs using the co-precipitation at low supersaturation method.
- Investigation of thermal decomposition of LDHs and formation of mixed-metal oxides.
- Reformation of mixed-metal oxides to layered structures using different aqueous media.
- Investigation of possible applications of reformed LDHs.

Statements Presented for the Defense

- Mg/Al, Co/Mg/Al and Ni/Mg/Al layered double hydroxides were synthesized using co-precipitation at low supersaturation method. The obtained LDHs could be easily thermally decomposed to the mixed metal oxides. The resulting oxides could be reformed to the layered structures in water and, to our knowledge, for the first time in magnesium nitrate medium.
- Partial substitution of magnesium by low amounts of cobalt or nickel does not show a strong influence on the formation of layered double hydroxide, but leads to different behaviour during thermal decomposition and regeneration as compared to Mg/Al containing LDH.
- Changes of cationic composition in LDH are observed during the reformation of mixed metal oxides in magnesium nitrate solution.

- The reformation medium and temperature influence the LDH crystallite size and the morphology of calcined LDH.

1. LITERATURE SURVEY

1.1. LAYERED DOUBLE HYDROXIDES

Layered double hydroxides, also known as anionic clays, hydrotalcite-like or hydrotalcite-type compounds are a family of layered materials. They have been a focus of recent books [2, 3, 7, 11, 19, 20], and reviews on catalysis [10, 12, 21-23] or physical characterization [24], or as reviews focusing on LDH nanocomposites with polymers [25, 26], and LDH intercalated with metal coordination compounds and oxometalates [27]. Most of the patents in this area concentrate on the use of LDH in the production of fine chemicals using various reactions. LDHs are also substantially used for polymerization reactions, as additives for cracking catalysts, as a support for dehydrogenation process, for the reduction of sulphur in gasoline. Other applications include NO_x removal, Fischer–Tropsh, partial oxidation of methane, water gas shift, H₂ production and a large variety of other uses in catalytic reactions [2, 10, 28]. Often LDHs are used as precursors for the production of other catalysts rather than as layered materials themselves. The nonstoichiometry of the mixed oxides and sometimes the reconstitution are the features of these materials which are very important in catalysis and which open a possibility for obtaining truly homogeneous catalysts. LDHs and mixed oxides derived after calcination were recently extensively explored for catalytic applications, with about 100 papers published each year. However most of the effort concentrated on the systems is with only one or two active components. The synergetic interactions of two or more active components that contribute to the catalytic activity seem to lack a comprehensive understanding, which is one of the prerequisites for the future rational design of more active LDH-based catalysts, particularly for applications in DeNO_x, DeSO_x, full oxidation of volatile organic compounds (VOC) and steam reforming reactions for H₂ production.

LDHs consist of hydroxide layers, containing usually two (or sometimes even more) different metal cations and possessing an overall positive charge, which is neutralized by the incorporation of exchangeable anions (Fig. 1.). In general, the materials also contain various amounts of water, hydrogen bonded to the hydroxide layers and/or to the interlayer anions. Metal cations are octahedrally coordinated by hydroxide groups, except the calcium aluminum hydroxide family. In the LDHs, the interlayer distance is variable, and may contract when the interlayer region is emptied or expanded in the presence of new anions or water molecules.

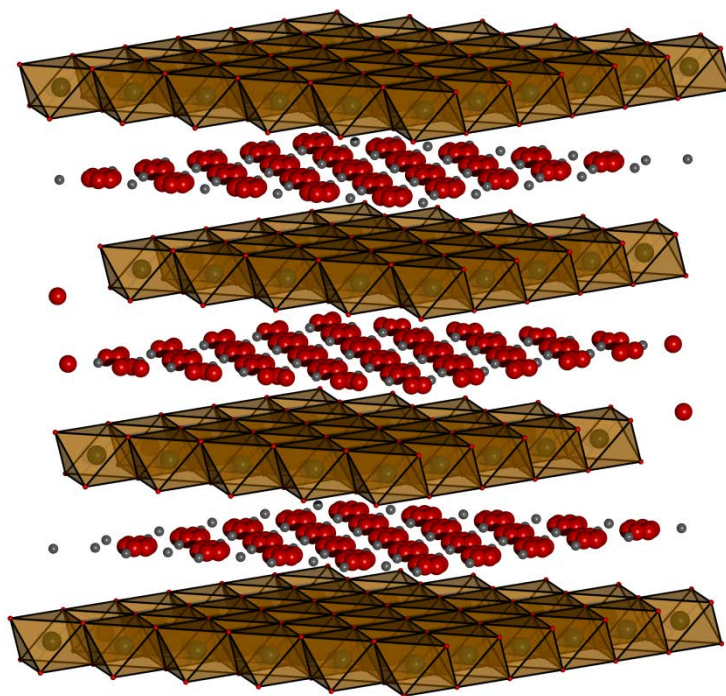


Figure 1. Schematic view of the structure of hydrotalcites. Bivalent and trivalent cations for example Mg^{2+} and Al^{3+} are six fold coordinated to form octahedra that share edges and form two-dimensional layers. Small spheres drawn in the interlayer region represent the compensating anions, usually CO_3^{2-} .

Some of these materials are found as natural minerals. All LDH minerals found in nature have a structure similar to that of hydrotalcite or its hexagonal analog, manasseite, and the majority adheres to the general formula $[M^{II}_x M^{III}_x (OH)_{2x}]^{x+} (A^{n-})_{x/n} \cdot mH_2O$, where M^{II} represents a divalent metal, M^{III} a trivalent metal, and A^{n-} an anion. The mineral hydrotalcite has the formula $[Mg_6Al_2(OH)_{16}]CO_3 \cdot 4H_2O$, which is usually written as $[Mg_{0.75}Al_{0.25}(OH)_2](CO_3)_{0.125} \cdot 0.5H_2O$ in order to emphasize its relationship to brucite. The brucite-like sheets stack on each other with respect to rhombohedral R3 symmetry, with the unit cell parameters being $a = 3.07 \text{ \AA}$ and $c = 3c' = 23.23 \text{ \AA}$ (c' is the thickness of one layer having one brucite-like sheet and one interlayer) [2].

1.1.1. Cations in LDH

The nature of the layer cations can be changed using a wide range of main group cations such as Mg, Ca, Al, Ga or In [29-31] or transition metal cations, such as Sc, Ti, V, Cr, Mn, Fe, Co, Ni, Cu, Zn, Y, Ru, Rh, Pd, Cd, La, Ir, Pt [1, 2, 32-41] normally in the divalent or trivalent state, although preparation of hydrotalcites with tetravalent cations such as V, Ti, Zr or Sn has been also reported [42-44]. The most frequent divalent metals have the ionic radii from 0.65 Å (Mg) to 0.80 Å (Mn) whereas the radii of the trivalent metals are usually between 0.50 Å (Al) and 0.69 Å (Cr) [2]. Metals which are not compatible with the octahedral sites of the brucite-type sheet, may be introduced in the interlayer space of these solids in their polyoxometalate form [45].

1.1.2. Anions in LDH

Regarding the anions in the interlayers, there are no strict limitations to their nature, and systems with many different anionic species have been described: simple inorganic anions such as carbonate, nitrate, sulphate and halogenides [2],

as well as organic dicarboxylate anions with varying carbon numbers or organic aromatic anions [46], metal complexes, low or medium-nuclearity oxometalates such as molybdate, chromate or vanadate [27, 47-51]. The number, the size, the orientation, and the strength of the bonds between the anions and the hydroxyl groups of the brucite-like layers determine the thickness of the interlayer. It has been reported in the literature that the common anion-exchange capability of the Mg-Al LDHs increases in the following sequence: $\text{I}^- < \text{Br}^- < \text{Cl}^- < \text{F}^- < \text{OH}^-$ for monovalent anions and $\text{SO}_4^{2-} < \text{CO}_3^{2-}$ for divalent anions [52]. The anion exchange selectivity in the Zn-Al LDHs follows the sequence: $\text{NO}_3^- < \text{Br}^- < \text{Cl}^- < \text{F}^- < \text{OH}^- < \text{CO}_3^{2-}$, obtained by the calculation of the Gibbs free energies [53]. The understanding of the influence of different intercalated anions in the LDH is important, because the anion exchange capacity can only be used when the introduced anion will have a higher affinity to the LDH layer than the precursor anion.

1.2. SYNTHESIS METHODS OF LDH

1.2.1. *Direct methods*

LDH compounds have been synthesized by direct methods, which include co-precipitation, sol-gel synthesis, hydrothermal growth, combustion synthesis, electrochemical synthesis and synthesis using microwave irradiation [7].

The most common method applied to preparation of hydrotalcite-like compounds is co-precipitation [2, 54]. The precipitating agents such as NaOH or NaHCO_3 are added to the prepared salts of the catalytically active materials and the support. As a result hydroxides or hydroxy salts precipitate and form a homogenous mixture that can be filtered. The morphology of obtained materials and the distribution of particle size depend on the supersaturation of the synthesis solution. Usually supersaturation is achieved by physical (evaporation) or

chemical (variation of pH) methods. For the preparation of LDHs, the method of pH variation is frequently used. The pH value must be chosen very carefully. If the pH is too low, not all different metal ions will precipitate, on the other hand, if the pH is too high, the dissolution of one or more metal ions may occur. Another point to note is that the pH value needed for the precipitation of HTs is not necessarily equal to the pH of the precipitation of the most soluble metal hydroxide. By using titration methods, it has been shown that, in the case of the Mg/Al system, the precipitation of the Mg/Al double hydroxide occurs in the pH range of 7.7-8.5, while the precipitation of $Mg(OH)_2$ occurs at pH 9.5, and that of $Al(OH)_3$ at much lower pH (4.0-4.5). The same effect is shown to occur in the Ni/Al system. The first precipitate constitutes the $Al(OH)_3$ (pH about 4), and then most of the nickel is precipitated in the mixed hydroxide form at a pH of about 5; whereas the precipitation pH of the pure Ni hydroxide is much higher [2]. Precipitation at low supersaturation is performed by slow addition of mixed solutions of divalent and trivalent metal salts with appropriate ratios into a reactor containing an aqueous solution of the desired interlayer anion. The conditions most commonly utilized are the following: pH ranging from 7 to 10, temperature 60-80 °C, low concentration of reagents and slow flow of the two streams. Washing is carried out with warm water, usually followed by some aging under the conditions of precipitation; the drying temperature should not exceed 120 °C. Low supersaturation conditions usually give rise to precipitates which are more crystalline with respect to those obtained at the high super saturation conditions, because in the latter situation the nucleation rate is higher than the crystal growth rate. A large number of particles is obtained, which, however, are usually small in size. Co-precipitation at high supersaturation may be carried out using the same equipment as the co-precipitation at low supersaturation. Using high supersaturation conditions the concentrations of the solutions are increased and/or the addition rate compared to the low supersaturation method. Usually prolonged washing is needed to reduce the amount of residual alkali because of the low

solubility of the alkali carbonates [2]. Factors that are considered important in the precipitation of the LDH compounds include the nature and ratios of the cations, the nature of anions, pH, temperature and aging.

Sol-gel method is known for its cost effectiveness and phase purity of the final product. The degree of crystallization and phase purity of layered double hydroxides prepared by sol-gel method strongly depend on the synthesis conditions, which should be more strictly controlled than in the co-precipitation method [55]. High-purity, well crystallized hydrotalcite was obtained rapidly by Paredes et al. [56]. Modification of the textural properties of the sol-gel synthesized LDHs is possible in convenient and useful ways with various and interesting possibilities [57, 58]. Another feature that makes these sol-gel derived materials distinguishable from those prepared by other synthetic methods is their high specific surface area [57].

Improved crystalline structures can be obtained by hydrothermal treatment in the presence of water vapour at temperatures not exceeding the decomposition temperature of the HT-like compound. Besides crystallinity, hydrothermal treatment can also be used to maintain or compensate for the required residual water that is lost in the previous stages of the LDH development. When co-precipitation for preparing LDHs fails, a combined co-precipitated and hydrothermal synthesis can be proposed to improve the crystallization. The hydrothermal crystallization is usually carried out at temperatures up to 200 °C under autogenous pressure for a time ranging from hours to days [59, 60]. While heating the reactants in a pressurized aqueous media improves the crystallinity of the resulting LDHs, hydrothermal synthesis may require additional effort and time. This method can also result in a decrease of surface area and growth of hydrotalcite crystals [59].

The preparation of Mg/Al hydrotalcite-like compounds by combustion synthesis has also been reported [61]. The method is based on the explosive decomposition of some organic fuels such as urea, glycine or saccharose. The

combustion method is a very rapid chemical process. The reaction is initiated and then promoted by the continuous thermal energy supplied to the precursor materials.

The synthesis of Ni/Al or Co/Al containing LDHs using a novel and simple electrochemical method has been reported [62-64]. The advantage of the proposed method is the short time needed to modify the electrode surface, whereas a drawback is that the electrodeposited material has a poor crystallinity. Unlike conventional deposition methods involving two-step processes, this new method consists of a one-step electrosynthesis of LDH phase on the surface of the foam in a very short time [62]. This way produces LDH films on large and irregular surfaces [63].

Microwave heating has also been used in the synthesis of several LDHs [41, 65-68]. Microwave irradiation under hydrothermal conditions leads to a very quick synthesis of LDHs and the ageing time is reduced from 18–24 h to 2–10 min. Moreover, hydrotalcites obtained by this method show smaller crystallite sizes and higher specific surface areas than samples, synthesized using aging of the gels at 150 °C for 24 h. [65]. Other authors have reported a crystallization rate enhancement of hydrotalcites, using microwaves [69, 70]. The specific surface areas of the mixed oxides obtained by calcinations at 450 °C of the conventionally prepared LDHs were higher than the microwave irradiated ones, but microcalorimetric and spectroscopic measurements upon CO₂ and CH₃CN adsorption showed that in the case of Mg/Al mixed oxides, the amount of both basic and acid sites is higher in the microwave irradiated LDHs. So it was concluded that the use of microwaves induces higher numbers of surface-defective sites [67, 68].

1.2.2. *Indirect methods*

Indirect methods include all synthesis routes that use LDH as a precursor. Examples of these are all anion exchange based methods such as direct anion exchange, anion exchange by acid attack with elimination of the guest species in the interlayer region and anion exchange by surfactant salt formation [71, 72]. The non-anion exchange methods include the delamination-restacking method and LDH reconstruction, reformation sometimes called the “memory effect” method.

The ion-exchange method is especially useful when the co-precipitation method is inapplicable. For example, when the divalent or trivalent metal cations or the anions involved are unstable in alkaline solution, or the direct reaction between metal ions and interlayer anions is more favorable. In this method, the guests are exchanged with the anions present in the interlayer regions of the formed LDH, resulting in specific anion pillared LDH. The diffusion of large anions into the interlayer space can be inhibited by reducing the basal spacing of the precursor. It is therefore difficult to intercalate large guest anions directly into the interlayer regions of LDHs. Species with low charge density comprise another class of guests, which are difficult to intercalate as a result of the reduced driving force associated with weakened interaction between the anions and the host layers. In such cases, pre-intercalation by smaller guests using co-precipitation or ion exchange methods is an effective way to enlarge the interlayer space, so that it is possible to introduce large or low charge target guests into the interlayer regions. The peculiarities of the anion exchange were studied for Mg/Al layered double hydroxide [52]. Small exchanged ions, such as NO_3^- or Cl^- , can be completely replaced by large anions, and an expanded layered structure with intercalated guest species is formed. In few cases, the intercalation of the sheets with anions creates freely accessible interlayer space. Only if such a permanent porosity is obtained, the materials can be considered as pillared anionic clays. All other compounds may simply be considered as intercalated layered double hydroxides [11].

Interestingly, calcined LDHs can recover their original layered structure if treated with water vapor, forming meixnerite-like materials, with interlayer hydroxide or in the case of contact with CO₂ hydrotalcite-like materials. This property has been used to prepare new LDHs. The initially formed mixed oxides should be immersed in solutions containing selected anions [12, 73-77] and/or cations [78-80]. In the literature the conversion of the periclase-like mixed metal oxides into layered double hydroxide has been termed as regeneration, reconstruction, restoration, rehydration, calcination-rehydration process, structural memory effect or simply memory effect. Recently, processes such as hydration, rehydration and reconstruction were well explained for Mg/Al hydrotalcite [81]. In this study, the term “reformation” is used to describe the process of the formation of LDH even with different chemical composition from the originally synthesized material. Such reformation has been observed for many studied systems [82, 83]. However it is not complete even after several days of equilibration and calcination of LDH at high temperatures [82]. It is also known, that LDHs containing transition metal cations are more difficult to recover. The use of microwave radiation as a heating source allowed to enhance the rate of reconstruction [84]. For successful reformation the choice of starting materials and temperature of calcination is very important. Total reconstruction occurs only in the same temperature range where the thermal decomposition was performed. At high temperatures, very stable M^{II}M^{III}₂O₄ spinel and M^{II}O phases are formed and the LDHs cannot be reconstructed. When the intercalation of anions occurs at the interlayer gallery region of LDH, the layered structure appears again. It was proved that the regeneration is a process of dissolution of mixed oxide and subsequent crystallization of LDH [74, 85]. The dissolution-crystallization mechanism of mixed oxide regeneration very well explains the formation of LDH with new anions and opens the possibility of changing the cation composition of LDH during the regeneration process. Some authors believe that regeneration occurs topotactically without the dissolution of the sample, hence the mechanism

of regeneration of LDH structure from mixed oxides remains an open subject [74, 86]. For Mg/Al hydrotalcite, the memory effect method was used to tune its basic properties [87]. Rehydration resulted in irregularly stacked platelets showing high activity as base catalysts due to their distorted edge structure [88]. The reformation property has been applied in the removal of anions in contaminated aqueous solutions [6, 89, 90], the immobilization of amino acids and enzymes to produce drugs [91], and in the insertion of new functionalities and active catalytic sites [27, 92]. Besides the above benefits, the memory of LDH can be also detrimental to the catalytic activity and stability, particularly in applications where LDH derived mixed oxides operate in wet streams at moderate temperatures [93]. The use of indirect synthesis is not only a way to get new materials but also a method to improve the properties of initially synthesized materials.

Reformation of LDH can provide several advantages. In the case of catalysts, it permits incorporation a third metal into the mixed oxide obtained upon thermal decomposition. Comprehensive studies of these layered double hydroxides are reported in the following sections.

1.3. PROPERTIES AND APPLICATION OF LDH

1.3.1. Properties of Mg/Al layered double hydroxide

In the mineral hydrotalcite with formula $[M^{II}_{1-x}M^{III}_x(OH)_{2x}]^{x+}(A^{n-})_{x/n} \cdot mH_2O$ the excess of positive charges on the hydroxide layers arise from the partial substitution of Mg^{2+} by Al^{3+} and can be compensated by ionic carbonate, which is the preferred anion found in natural hydrotalcites. The most popular HT is the stoichiometric double magnesium–aluminium hydroxide with the formula $Mg_6Al_2(OH)_{16}CO_3 \cdot 4H_2O$. The degree of partial substitution of Mg^{2+} by Al^{3+} noted as x in the general formula can vary in the range of 0.1–0.5 [11] giving rise to the family of Mg–Al hydrotalcites. It has been stated that the range for pure

phases is restricted to 0.2–0.33, since for higher or lower values of x , other compounds like pure hydroxides or carbonates were obtained [2]. The structure and surface properties of Mg-Al hydrotalcites and the resulting mixed oxides strongly depend on the chemical composition and synthesis procedures. The surface area, intimate contact between two or more oxide components and the size of the resulting metal oxide clusters strongly influence the rate and selectivity of chemical reactions in the catalytic processes. In the samples with low Al content ($x < 0.2$) the basic site density is lower compared to pure MgO. At higher Al contents ($0.2 < x < 0.5$) a highly interacting Mg-Al oxide phase is forming. Al^{3+} ions incorporate into the MgO matrix and increase the concentration of surface defects. In the samples with $x > 0.5$ demixing of the Mg-Al phase occurs leading to the formation of bulk MgAl_2O_4 spinels. As a result, the density of basic sites diminishes [94]. Calcined hydrotalcite with low Al content showed higher activity than pure MgO in the double-bond isomerization of 1-pentene [95]. It has been reported that the participation of both acidic and basic sites is required for alkylation reactions and that surface acid-base properties are determined by the Al content [96].

Fresh hydrotalcites are highly hydrated materials. Water content in fresh HT depends on the preparation temperature, water vapour pressure and the nature of the anion. HTs containing nitrate or carbonate anions can already lose one third of their interlayer water at 100 °C. Thermogravimetric analyses revealed successive steps of weight loss with increasing temperature. The asymmetric shape of the DTG curve in the dynamic thermal analysis experiment indicated the existence of two types of interlamellar water molecules, those that are free or bonded to other water molecules and those solvating the anion species and hydroxide. Decomposition of the hydrotalcites occurs in three steps: (i) evaporation of adsorbed water appears up to 100 °C; (ii) elimination of the interlayer structural water up to 250 °C; (iii) dehydroxylation and decarbonation of the hydrotalcite framework up to 600 °C [97]. A significant rearrangement of the octahedral

brucite-type layer occurs with migration of the Al cations out of the layer to the tetrahedral sites in the interlayer. Upon heating up to 400 °C the anions in the interlayer are decomposed, and the material is completely dehydroxylated. The X-ray diffraction measurements confirmed this sequence and showed a decrease of basal spacing after the dehydration and a collapse of the layered structure upon the decomposition, along with the appearance of a pattern resembling the rock salt structure [98]. However, the Al and Mg coordination changes during the heat treatment. The *in situ* and *ex situ* experiments showed different results, indicating the importance of *in situ* technique. Although some controversy exists concerning the temperatures at which the changes in the HT structure occur, there is a common consensus that the adsorbed and interstitial H₂O is removed from the interlayer and dehydroxylation at the cation layers occurs creating less coordinated Al centers. ²⁷Al MAS NMR spectroscopy recorded at elevated temperatures indicated that this process occurs already at temperatures above 100 °C. Simultaneous investigation using *in situ* XAFS at the Mg and Al K-edges showed that the coordination of Al is lowered at a temperature of 152 °C. However, these changes are reversible after cooling down the samples to the room temperature. At temperatures above 202 °C, the actual dehydroxylation process commences and changes of both the Mg and Al coordination were observed. These dehydroxylation processes were no longer reversible. At 202 °C, the Mg-OH bonds start to break and the coordination of the Mg centers is altered by the formation of new Mg-O-Mg bonds. This process is accompanied by the evolution of H₂O from the sample. At this temperature, the formation of a rock salt MgO-like phase starts to occur [83]. This range between the temperature of decomposition of hydrotalcite and the formation of spinel is very interesting, since here the metastable and generally poorly crystallized phases can be formed. In the literature, these phases have been referred to under many different names like NaCl-type mixed oxides, spinel-type phases, mixed metal oxides, mixed oxide solution or simply mixed oxides. However, all authors agree that mixed oxides have

disordered structures, containing an excess of divalent cations in comparison to the stoichiometric spinels [2, 11]. The addition of an excess water during the rehydration at room temperature fully reverses the changes in the coordination of the hydrotalcite even calcined at 452 °C. X-ray diffraction analyses revealed the changes in the 003 and 006 reflections of HT at about 182 °C, showing a decrease in the interlayer distance. This was attributed to a loss of interstitial H₂O. However, since the Al and Mg coordinations are already changing at low temperatures, it was concluded that structural changes take place in the interlayers as well as inside the Mg-Al hydroxide layers. At higher temperatures decarboxylation occurs, which is accompanied by the formation of a MgO phase. The latter process is accompanied by a loss of the lamellar arrangement of the layers. The structures formed after calcination HT at 520 °C still exhibited the memory effect, although the restoration of the HT layered structure is much slower. After calcination-rehydration cycle no new Mg and Al coordination modes were observed by Mg and Al K-edge XAFS. The Mg and Al coordinations were completely restored to the original hydrotalcite structure [83].

The gas phase hydration of the calcined hydrotalcite back into a layered structure was also investigated by *in situ* XRD. At 30 °C the metal oxide gradually transformed into the meixnerite. The intensity of the meixnerite phase increased with the time of exposure to water vapor. In contrast to the original hydrotalcite, containing mainly carbonate ions as charge balancing anions, the layer charge in meixnerite was only compensated by hydroxide ions [81]. The transformation of the intermediate dehydrated phase (at 200 °C) back to hydrotalcite and the reconstruction of the calcined Mg/Al hydrotalcite at 450 °C was investigated by *in situ* XRD [99]. The sample was cooled and then contacted with moisturized N₂. The recovery of the hydrotalcite from dehydrated phase was very fast in the first 5 min in the H₂O-containing flow at 30 °C. The rehydration involves not only the physical filling of the interlayer space by water molecules but also a phase transition from the disordered, dehydrated, layered phase back to the original

hydrotalcite. It was shown that the interlayer of the rehydrated product can accommodate more water than the as-synthesized HT [99]. From the *in situ* XRD results, it was indicated that reconstruction of calcined hydrotalcite does not go through the layered dehydrated phase. The interlayer spacing was almost identical to that in the as-synthesized sample during the whole reconstruction process. This observation indicates that the retrotopotactic transformation occurs in a single step (mixed oxide \rightarrow meixnerite), in contrast with the two-stage transition during the decomposition (hydrotalcite \rightarrow dehydrated layered phase \rightarrow mixed oxide). In view of this, hydroxylation of the oxide structure and filling of the interlayer space by water are simultaneous, contrarily to the sequence in thermal decomposition. By means of energy-dispersive X-ray diffraction (EDXRD) Millange et al. [85] determined that 3 h was sufficient time to complete the reconstruction of calcined hydrotalcite (at 400 °C) in Na₂CO₃ aqueous solution at room temperature. This process was accelerated by increasing the temperature, since dissolution of the poorly crystalline oxide in solid carbonate and nucleation of the reactive species occurs faster. The reconstruction time and degree of reconstruction have pronounced effect on the structural and catalytic activity of hydrotalcites. Calcined hydrotalcites stirred with water vapour or de-carbonated water under inert atmosphere form a highly active solid base catalyst. In this case, the restoration of the original layered structure occurs with hydroxyl groups as charge balancing anions in the interlayer space instead of carbonate anions [52]. The absence or presence of steam showed no effect on the activation of hydrotalcites and lead to identical decomposition behaviour with respect to dehydration, dehydroxylation, and decarbonation processes. The particle morphology and average crystallite sizes of the resulting oxides were also very similar. However, steam activated mixed oxides had lower surface area and pore volume compared to dry decomposed hydrotalcite [100]. Being solid inorganic bases, calcined HTs are recognized as thermally stable and potentially recoverable and recyclable catalysts. Activation of Mg/Al hydrotalcites via thermal treatment followed by

rehydration resulted in irregularly stacked platelets showing high activity as base catalysts due to the distorted edge structure of the platelets [88]. Variations in compositions and formation of mixed oxides with high catalytic activity makes hydrotalcite still an interesting material for investigations.

1.3.2. Application of Mg/Al LDH

Since hydrotalcites have a well-defined layered structure with nanometer interlayer distances (0.3–3 nm) and contain important functional groups, they are widely used as adsorbents for liquid ions and gas molecules [2]. The interlayer anions may be exchanged with anions in external solutions, therefore HT can be applied for the removal of anionic toxins during water purification [6, 101]. The ability of HT to adsorb inorganic as well as organic anions makes these materials very attractive for many applications. They also find use as catalysts for oxidation, reduction and other catalytic reactions. Hydrotalcite can be applied to the preparation of composite materials like supported anion catalysts, recovery of precious anionic compounds [27]. HTs have been also used in the plastics industry [102]. The hydrotalcites intercalate bioactive molecules with negative charges into the interlayers forming bio-HT nanohybrids. The bio-nanohybrids are electrically neutral and can be transferred into biocells and organs through cell membranes [103, 104]. Hydrotalcites are good candidates for CO₂ capture. Carbon dioxide is an acidic molecule and can adsorb on the basic solids [8, 105]. Hydrotalcite inorganic membranes show good promise for application in sensor devices and in membrane reactors for the production of hydrogen through the steam reforming or the water gas shift reactions [106]. Recent studies have shown that EVA polymer filled with 50 wt.% of hydrotalcite has slow heat release rate and the lowest evolved gas temperature. The layered structure may play a key role in this respect [105]. Kyowa Chemical Industries of Japan demonstrated that adding Mg/Al HT to PVC in combination with other additives such as zinc stearate and tin maleate

lead to an enhancement in thermal stability of the resin [107]. The mixed oxide obtained by thermal decomposition exhibits much higher basic properties than fresh HT. Mixed metal oxides have also a potential to be used as new bifunctional catalysts with a unique combination of acid–base and redox properties. Thermal activation of hydrotalcites is reported as an efficient preparation method for catalysts used in transesterification, alcohol elimination and condensation reactions [108]. Supporting the hydrotalcite over the carbon nanofibers allows to produce highly active base catalysts [109], which are of general importance for organic synthesis and fine chemicals manufacturing.

The Mg/Al hydrotalcite is the mostly studied layered double hydroxide and in this study was used as a reference sample.

1.3.3. Properties of Co/Mg/Al layered double hydroxide

As mentioned previously a wide range of derivatives containing various combinations of M^{II}, M^{III} and A ions in layered double hydroxide $[M^{II}_{1-x}M^{III}_x(OH)_{2x}]^{x+}(A^{n-})_{x/n} \cdot mH_2O$ can be synthesized. A number of cobalt containing LDHs where Mg is replaced by cobalt has been prepared [110-113]. Xu and Zeng [114] have synthesized monometallic cobalt hydrotalcites in order to obtain Co₃O₄ spinels. In other cases Co has been added as a second or third metal [115-117]. Co/Mg/Al layered double hydroxides show a unique layered structure. The evolution of the lattice *a* parameter with the cationic composition provides evidence that Co²⁺, Mg²⁺, and Al³⁺ are combined in the same layer. The crystallinity of LDH depended on the amount of Co²⁺ and/or Mg²⁺, probably due to their respective ionic radius [115]. The isomorphous replacement of Co²⁺ by Mg²⁺ showed effect on the amount of interlayer water due to the well-known ability of these cations to be hydrated. Higher thermal stability of samples containing low amount of cobalt were explained by the higher local charge density of the layers or to the higher affinity of Mg²⁺ towards CO₃²⁻ [115].

Co/Mg/Al oxide derived from LDHs showed high surface area. In those samples, cobalt seemed to be present not only as isolated and well dispersed paramagnetic ions but also as some kind of very small Co-containing particles with an internal antiferromagnetic ordering at low temperature [14]. Calcined Co/Mg/Al layered double hydroxide forms $\text{Co}_x\text{Mg}_{1-x}\text{Al}_2\text{O}_4$ solid solutions having the spinel structure and various cationic distributions. The nature of cations and the temperature of activation either induce the formation of monophasic solid solutions with rock salt or spinel-like structures or segregation of several phases [2]. The Co/Al and Mg/Al LDHs behave differently during the thermal treatment. It has been shown that DTA curve of the Co/Al LDH displays two similar endothermic maxima as the Mg/Al hydrotalcite, just the second peak appears at much lower temperature [112]. The LDHs containing all three cations (Co, Mg, Al) show different decomposition profiles compared to the binary composition. The DTG shows two peaks corresponding to the dehydration and dehydroxylation/deanation steps. The decomposition temperature of Co/Mg/Al system is higher than that of Co/Al LDH, but lower than that of Mg/Al LDH [118]. The best conditions found to preserve the cobalt species in the divalent oxidation state are preparation of the samples at controlled pH and then ageing them under microwave irradiation. Thermal decomposition in nitrogen atmosphere stops the oxidation to Co^{3+} species, which was observed in oxygen or air [111].

Cobalt containing LDHs or their derived oxides are often treated with reducing gases such as H_2 , CO or CH_4 in order to convert Co^{2+} and Co^{3+} to metallic or metallic-like species that can serve as active sites in catalysis. The main reduction of cobalt cations occurs above 600 °C [117]. A great advantage of this process is the very fine dispersion of the metallic or metallic-like species on the oxide support. The reducibility of the metal cations depends on the type and ratio of cations, formation of spinels, and temperature.

As reported previously, detailed reconstitution/reformation studies are practically limited to the Mg/Al systems. It has just been shown, that Co/Al

layered double hydroxide does not easily recover the original structure. The mixed oxide formed upon thermal treatment at 200 °C in air was shown to be remarkably stable. This oxide was kept for 30 days in a wet gas (5 vol% H₂O in N₂) flow or for 12 h in an aqueous solution of 0.5 M Na₂CO₃ [119]. Partial oxidation of Co²⁺ to Co³⁺ together with the thermodynamic stability of the formed solid solution phase is believed to be the main reason for the difficult reconstruction after decomposition of the LDH at such low temperatures. The main Co₃O₄ phase intimately dissolves the Al³⁺, forming a very homogeneous and stable solid solution. The presence of Al in the spinel phase at such low temperatures supports the high resistance against reconstruction. LDH intercalated with Co/Mg/Al acetate showed different behavior compared to Co/Al and Mg/Al systems after decomposition and reconstruction. Partial reconstruction was observed in the LDH structure that was decomposed at 800 °C and no reconstruction was seen for the sample that was treated at ≥ 1000 °C [118]. Once the stable spinel phase is formed it will not hydrolyze to give back the LDH. It has been shown that Co/Mg/Al system with lower loadings of cobalt forms only Mg(Al)O mixed oxide phase after calcination at 750 °C [120], avoiding the spinel formation which could influence the reformation of LDH with cobalt in the structure. In this study this possibility will be investigated using different media for the reformation.

1.3.4. Application of Co/Mg/Al LDH

The decomposition temperature and the reconstruction conditions play a crucial role in the application of these materials in catalysis. The finding that Co/Al LDH is stable in a wet feed gas, justifies its application as a catalyst in such conditions. An interesting way to obtain mixed cobalt catalysts is through the use of LDHs as precursors [2, 115]. Catalysts from cobalt containing LDHs were tested in the oxidative steam reforming reaction of ethanol under autothermal conditions. Co-catalyst reached a higher H₂ production level at lower temperatures

compared to the Ni-one [121]. LDHs with cobalt are used as precursors for the preparation of Fischer–Trops catalysts [122, 123], for hydrogenation of nitriles [116] and for the synthesis of carbon nanotubes [124]. The selectivity and conversion of these catalysts depend on the preparation method, cobalt concentration and the type of ageing process. Cobalt based catalysts were synthesized using the memory effect of LDHs. Their activity for VOC oxidation was investigated. The high activity was explained by a high quantity of cobalt species reduced at low temperature. The solid obtained by reconstruction was then decomposed and activated, and was shown to be active in toluene oxidation [78]. Cobalt containing LDH after calcination and reduction showed high catalytic activity in removal of SO_x (SO_2 and SO_3) and NO_x (N_2O , NO and NO_2). Mixed oxides obtained from the Co/Mg/Al LDHs were investigated in a simultaneous removal of NO_x and SO_x [13, 14]. The NO_x storage/reduction (NSR) technology is based on the selective storage of NO_x as nitrates under lean (oxidizing) conditions and their non-selective reduction under the short, rich (reducing) excursions [125]. NSR catalysts are typically composed of at least one basic compound (alkaline or alkaline-earth oxides) and at least one precious-metal component. One of the most common formulations used is Pt and Ba supported on Al_2O_3 [126]. The problem of this material is its fast poisoning by sulphur compounds and its low activity at low temperatures. In this study the influence of reconstitution/reformation of cobalt containing LDH on their properties in NO_x removal will be investigated.

1.3.5. Properties of Ni/Mg/Al layered double hydroxide

There are several papers describing the synthesis of Ni/Al LDH called takovite [1, 55, 112, 127, 128]. In other cases Ni is added only as a second or third metal to the hydrotalcite-type material [17, 33, 129]. Co-precipitation of different compositions leads to the pure hydrotalcite phase with different cell parameters.

When the isomorphic substitution of Mg^{2+} with Ni^{2+} cations is performed, the lattice parameter a may decrease, because it mainly depends on the ionic radii of the cations in octahedral coordination ($\text{Mg}^{2+} > \text{Ni}^{2+}$) [33]. The difference in c parameters between various LDHs can be attributed to different Coulombic attractive forces between the positively charged brucite-like layer and the anion located in the interlayer region. After calcination at 900 °C oxide-type and spinel-type phases segregate and Ni is distributed among NiO, $(\text{Ni,Mg})\text{Al}_2\text{O}_4$ and NiO–MgO phases. However, this strongly depends on composition [15]. Partial substitution of Mg by Ni ions resulted in a different thermal decomposition of LDH. The DTG pattern of Ni/Mg/Al hydrotalcite is characterized by a sharp minimum at 198 °C, which was attributed to the removal of the interlayer and physisorbed water and by an asymmetric peak at 376 °C with a small shoulder at the high temperature side (about 500 °C) related to the thermal decomposition of hydroxyl, carbonate and nitrate anions [117]. The oxide morphology is also affected by the divalent cation. Upon thermal treatment, the presence of nickel induces the transformation of the characteristic platelets in the as-synthesized clays into nodular particles. Most importantly, the divalent cation determines the ability of the resulting oxide to exhibit memory effect. In contrast with the facile reconstruction of Mg/Al oxide, no sign of recovery was observed in Ni-Al oxide upon exposure to water vapour at room temperature. Rehydration of the Ni/Mg/Al layered phase was not fully reversible [130]. The reconstruction of layered structure for Ni/Al compounds was obtained using strong basic media and microwave hydrothermal treatment. However, when a larger Ni/Al ratio was used or the process was carried out in water or aqueous NH_3 solution the reconstruction did not proceed [84].

The compounds with high Ni contents require mild reduction conditions due to the formation of large NiO crystallites. Contrary, catalysts with lower Ni contents are stable under reaction conditions. This is due to the insertion of the Ni^{2+} species into the NiO–MgO solid solution. Moreover, a significant reduction in coke

formation is observed, although a harsher reduction treatment is required to activate the catalyst [15]. In this study the possibility to reform ternary Ni/Mg/Al LDH at different conditions will be discussed.

1.3.6. Application of Ni/Mg/Al LDH

Ni/Mg/Al LDH was chosen due to its good catalytic activity in gasification, catalytic partial oxidation and steam reforming [15-18]. The nickel-aluminum mixed oxides resulting from the thermal decomposition of hydrotalcite-like coprecipitates are among the most studied catalyst precursors for steam-reforming [17, 63, 131-133]. The interest in these oxides is due to remarkable properties of the final catalysts, such as a high metallic dispersion and high particle stability under extreme conditions [127]. It has been shown, that the improved performance of Ni/Mg/Al mixed oxide catalysts was related to the incorporation of MgO and Al₂O₃ into the MgAl₂O₄ phase, which reduced nickel incorporation into the supports leaving nickel in its active form [131]. In other work, it was reported that the compositions containing Mg showed higher catalytic activity than those without Mg, as well as a significant reduction in the amount of deposited carbon [134]. Nickel based catalysts derived from thermal decomposition of the Ni/Mg/Al hydrotalcite-like precursors prepared by a coprecipitation method exhibited high activity and stability and long lifetime in steam reforming of methane at a residence time of milliseconds. The catalytic performance was greatly improved in comparison to the traditional Ni catalysts. This type of catalyst was even compared to Rh catalyst and the results were very similar despite the fact that the residence time was only tens of milliseconds [135]. The catalytic performance of fresh and regenerated Ni/Mg/Al catalysts was compared for CH₄ steam reforming. Thanks to the stabilization of MgO on Ni particles and the high removal rate of carbon deposits, the regenerated catalyst showed improved H₂ production [93]. Ni/Mg/Al systems showed good catalytic

performance for the hydrogenation of nitriles into primary amines [136], and in the gas phase hydrodechlorination reaction of 1,2,4-trichlorobenzene [137]. Volatile organic compounds emitted from many industrial processes and transport vehicles significantly contribute to atmospheric pollution, and the catalytic total combustion is one of the most effective and economically attractive treatments. Ni/Mg/Al mixed oxides prepared from the LDH precursors were tested as catalysts for the total combustion of some commonly encountered VOC, such as toluene, methane and ethanol [138, 139]. Gasification of biomass with air produces a dirty raw gas composed of a mixture of H₂, CO, CO₂, H₂O, CH₄, light hydrocarbons, tars, NH₃, some dust and other trace components. For most applications, this gas has to be cleaned of at least dust and tars. Nickel-based supported catalysts, used extensively in the petrochemical industry, have shown high activities for tar reforming/decomposition and ammonia decomposition in coal and biomass gasification. When used as secondary catalysts, the supported nickel catalysts could attain nearly complete decomposition of both tar and ammonia at > 800 °C [140]. Nickel containing LDH was used to investigate reformation effect of layered double hydroxide in gasification gas cleaning application herein.

2. EXPERIMENTAL

2.1. MATERIALS

Layered double hydroxides were synthesized using Al(NO₃)₃•9H₂O, Mg(NO₃)₂•6H₂O, Ni(NO₃)₂•6H₂O, Co(NO₃)₂•6H₂O, NaOH, NaHCO₃ from Lach - Ner, s.r.o. (Neratovice, Czech Republic) as starting materials. Gibbsite Al(OH)₃ from Pikalevsky Glinozem Joint-Stock Company was used for the preparation of gasification gas cleaning catalyst. Deionised water was used for all synthesis, solutions preparations and washing. The gases used in activity studies were supplied by AGA Ltd. (>99% purity). A mixture of 90 w-% toluene (>99.5%

purity, VWR International) and 10 w-% naphthalene (>99% purity, VWR International) was used as the model system for tar.

2.2. SYNTHESIS AND POST-SYNTHESIS MODIFICATIONS

2.2.1. *Mg/Al LDH*

The layered double hydroxide with natural hydrotalcite composition was prepared by co-precipitation under low supersaturation from a solution of the appropriate metal nitrates with a molar ratio of Mg:Al = 3:1 and solution prepared from NaHCO₃:NaOH (1:2). The solution of metal nitrates was slowly added to the solution prepared with NaHCO₃+NaOH (pH ≈ 12) under vigorous stirring. After mixing, the obtained sample was aged at 80 °C for 6 h. The resulting slurry was filtered and washed with distilled water and dried at room temperature (sample was labeled as Mg/Al). The mixed-metal oxide was obtained by heating the synthesized Mg/Al specimen for 3 h at 650 °C and was labeled as Mg/Al₆₅. The hydration of mixed-metal oxide was carried out at 20 °C for 6 h with continuous stirring in deionised water pH ≈ 6 (2 g of mixed oxide in 40 mL of water) and the sample was denoted as Mg/Al_{W20}. The regeneration in 1 mol L⁻¹ magnesium nitrate solution with pH ≈ 3.7 was performed under the same conditions (2 g of mixed oxide in 40 mL of 1 mol L⁻¹ Mg(NO₃)₂) and the sample was denoted as Mg/Al_{N20}. The influence of regeneration temperature was investigated in the same solutions at 80 °C. The sample hydrated at 80 °C was named as Mg/Al_{W80} and regenerated one in Mg(NO₃)₂ solution at the same temperature was named as Mg/Al_{N80}. Schematic presentation of synthesis and post-synthesis modifications of Mg/Al LDH are shown in Fig. 2.

2.2.2. *Co/Mg/Al LDH and Ni/Mg/Al LDH*

Layered double hydroxides containing cobalt or nickel were prepared under the same conditions as the Mg/Al sample, except that 15% of 1 mol L⁻¹

magnesium nitrate solution was replaced by 1 mol L⁻¹ cobalt nitrate solution or 1 mol L⁻¹ nickel nitrate solution. The obtained samples were named as Co/Mg/Al and Ni/Mg/Al, respectively. After decomposition at 650 °C (Co/Mg/Al₆₅ and Ni/Mg/Al₆₅), the hydration was performed in water at 20 °C and 80 °C for 6 h and regeneration in Mg(NO₃)₂ solution at the same temperatures. The samples containing cobalt were named as Co/Mg/Al_{w20}, Co/Mg/Al_{w80}, Co/Mg/Al_{N20}, Co/Mg/Al_{N80}, and the specimens containing nickel were named as Ni/Mg/Al_{w20}, Ni/Mg/Al_{w80}, Ni/Mg/Al_{N20}, Ni/Mg/Al_{N80}, respectively. After the reformation processes, the samples were washed with water and dried in air. Schematic presentation of synthesis and post-synthesis modifications of LDH with nickel or cobalt are shown in Fig. 2.

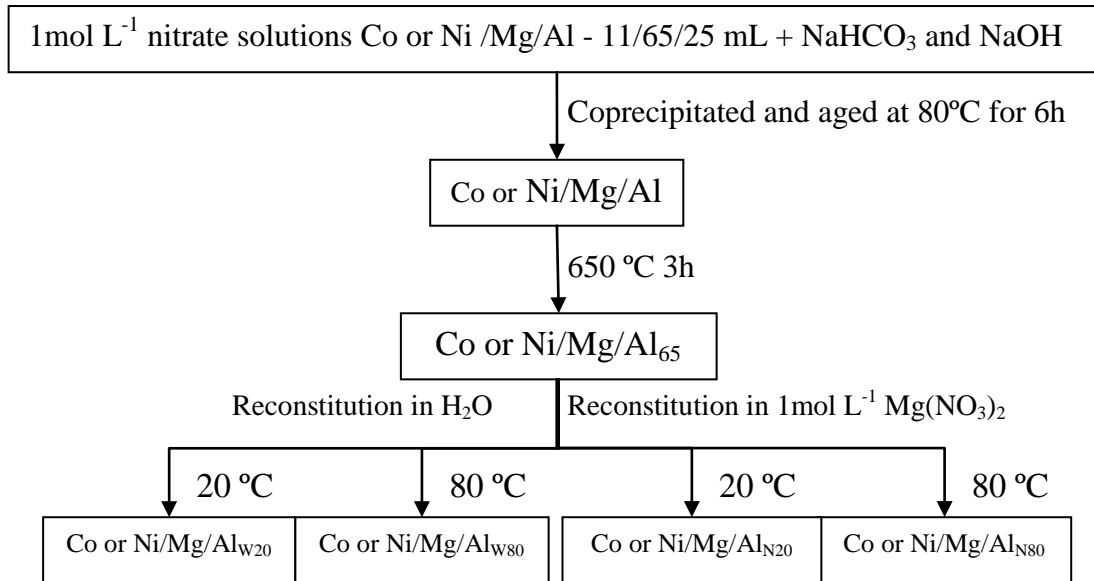


Figure 2. Chart of synthesis and post-synthesis modifications of LDH samples. Mg/Al LDHs were synthesized without cobalt or nickel nitrate solutions.

Two cobalt containing LDH samples were chosen for NO_x removal application. Co/Mg/Al sample was synthesized by co-precipitation under low supersaturation as described previous, only the aging time was changed to 24 h.

The prepared powder was crushed and sieved to obtain the fraction with a particle size of 0.2-0.5 mm. One sample was calcined at 650 °C for 3 h and then left in air at room temperature and humidity. This reformed sample was named Co1. The other sample was tested right after thermal treatment to avoid reconstitution and the sample was named Co2.

Catalysts for decomposition of tar, ammonia, and methane were synthesized according to Norta Ltd technology. The Mg/Al hydrotalcite synthesized as described previously was deposited on the gibbsite core. The powder was subsequently heated at a rate of 1.67 °C/min to 650 or 850 °C and calcined for five hours to yield two powders. The calcined powders were dipped into an aqueous 1 M solution of nickel (II) nitrate for 45 min, and thereafter washed with distilled water and dried. Reformation of decomposed layered double hydroxide was used to introduce nickel. Finally, the powders were heated at a rate of 5 °C min⁻¹ to 850 °C and calcined for five hours to obtain two powder form catalysts: Ni1 (intermediate calcinations temperature 650 °C) and Ni2 (intermediate calcinations temperature 850 °C).

2.3. CHARACTERIZATION

The XRD patterns of the synthesized, calcined and regenerated samples were recorded with a conventional Bragg-Brentano geometry ($\theta - 2\theta$ scans) on a DRON-6 automated diffractometer equipped with a secondary graphite monochromator. Cu K α radiation ($\lambda = 1.541838 \text{ \AA}$) was used as a primary beam. The patterns were recorded from 5 to 70° 2θ in steps of 0.02° 2θ , with the measuring time of 0.5 s per step. Silicon was used as a reference sample. The cell parameters c and a of the rhombohedral structure were determined from the positions of the (003), (006) and (110) diffraction lines, respectively. The lattice parameter $a = 2d(110)$ corresponds to an average cation–cation distance calculated from the 110 reflection, while the c parameter corresponds to three times the

thickness of $d(003)$ parameter. In this case c was calculated from two diffraction lines using equation $c = 3/2 [d(003)+2d(006)]$. The average crystallite sizes of layered double hydroxides were calculated from the 003, 006 and 110 reflections, using the Debye-Scherrer equation.

Simultaneous thermal analysis (STA: differential scanning calorimetry – DSC, thermogravimetry – TG and differential thermogravimetry – DTG) was employed for measuring the thermal stability and phase transformation of synthesized products at a heating rate of $10\text{ }^{\circ}\text{C min}^{-1}$. The temperature ranged from $30\text{ }^{\circ}\text{C}$ up to $900\text{ }^{\circ}\text{C}$ under air atmosphere. The test was carried out on a Netzsch instrument “STA 409 PC Luxx”. Ceramic and Pt-Rh crucibles were used as sample holders.

Metal loadings of the layered double hydroxides were analyzed by X-ray fluorescence technique (XRF) on a Spectro Analytical Instrument GmbH&Co.KG. with a Pd window X-ray tube. The analysis was carried on a 32 mm disc. XRF apparatus uses the Turboquant calibration method that is able to analyze all elements from Na to U. Mean values of relative standard deviation for analysed elements were: Mg – 1.54%; Al – 1.42%; Co – 3.7% and Ni – 2.4%.

The surface morphology of the synthesized and regenerated samples was studied by scanning electron microscope (SEM) EVO 50. The analysis of images was done with the ImageJ software.

Surface areas, pore volume and pore size distribution of the samples calcined at $650\text{ }^{\circ}\text{C}$ for 3 h were estimated using the Brunauer–Emmet–Teller (BET) [141] and Barret-Joyner- Halenda (BJH) equations [142]. Prior to analysis, calcined nickel containing layered double hydroxides were outgassed at $400\text{ }^{\circ}\text{C}$ overnight. The measurements were carried out on a Micromeritics ASAP 2010 instrument by nitrogen adsorption at $-198\text{ }^{\circ}\text{C}$. Cobalt containing samples were outgassed at $250\text{ }^{\circ}\text{C}$ for 5h. Samples were analyzed with Quantachrome Autosorb-1C equipment using the program Autosorb.

2.4. ACTIVITY STUDIES

The NO_x removal reaction experiments were carried out in a fixed bed, tubular reactor (22 mm diameter and 530 mm length). In the experiments, 1 g of catalyst in the form particles of 0.2–0.5 mm, was introduced in to reactor and was pre-treated for 1 hour in nitrogen at 450 °C and in H₂ at the same temperature for 30 min. Afterwards, the desired reaction temperature was set and the reaction feed admitted. This consists in 650 mL min⁻¹ of a mixture composed by NO, C₃H₈, oxygen and balanced with nitrogen. Catalytic tests were set at a space velocity of 20.000 h⁻¹, using a cyclic sequence of changes in the feed composition, simulating car exhaust emissions in:

- lean conditions 120 s: 13% O₂, 530 ppm NO_x, 50 ppm C₃H₈, N₂ balance;
- rich conditions 60 s: 8% O₂, 530 ppm NO_x, 700 ppm C₃H₈, N₂ balance.

After evaluating the behaviour during a sequence of seven lean–rich cycles at a given temperature, the reactor temperature was raised to another temperature under N₂ where the behavior was further monitored over the cycle series. The NO_x present in the gases from the reactor were analyzed continuously by means of a chemiluminescence detector Rosemount 951A.

The activity tests of the catalysts in the decomposition of tar, ammonia and methane from the synthetic gasification gas were performed at atmospheric pressure in quartz reactors. The reactor was packed with a powdered catalyst and placed inside a three-zone furnace. In the activity tests of catalysts, 0.1 g of 225–300 µm particle size powder was packed onto the quartz grid of the tubular quartz reactor (inner diameter 10 mm). In the first experimental set, catalyst samples were pre-reduced under a gas flow of 20 vol-% of H₂/N₂ by increasing from ambient temperature to 800 °C at a rate of 5 °C min⁻¹ and keeping it there for 1 h. In the second set, the samples were tested without pre-reduction. The catalysts were studied in the clean-up of a synthetic gasification gas at 700 and 900 °C with and without sulfur addition. The gas feed rate was adjusted to 1000 mL min⁻¹

(NTP) for the powder form catalyst tests, giving a space velocity of $27,000 \text{ h}^{-1}$. All the gas lines were heated up to $200 \text{ }^\circ\text{C}$ to avoid condensation. The mixed feed comprised 12.5 vol-% CO, 15.0 vol-% CO_2 , 11.0 vol-% H_2 , 6.0 vol-% CH_4 , 1.0 vol-% C_2H_4 , 0.5 vol-% NH_3 (in N_2), 3.4 vol-% O_2 , 50.6 vol-% N_2 , $15 \text{ g m}_\text{N}^{-3}$ tar model compound, and $110.0 \text{ g m}_\text{N}^{-3}$ H_2O . The catalysts were first studied without sulfur addition. Hydrogen sulfide (in N_2), 100 ppm, was then added to the feed stream to mimic the sulfur impurities of the gasification gas.

The inlet and outlet gases were analyzed with a Gaset FTIR gas analyzer. The condensable compounds were removed from the product gas by a cold trap consisting of isopropanol and water in series on an ice bath. The flow rate and temperature of the dried product gas were measured with a dry gas flow meter and it was directed into a Sick Maihak type S710 on-line gas analyzer, wherein the volumetric composition of the dry gas (CO , CO_2 , CH_4 , O_2 and H_2) was measured.

3. RESULTS AND DISCUSSIONS

3.1. SYNTHESIS OF LDHs BY COPRECIPITATION METHOD AND X-RAY CHARACTERISATION

All three layered double hydroxides Mg/Al, Co/Mg/Al and Ni/Mg/Al were successfully synthesized by co-precipitation method. As seen from the XRD

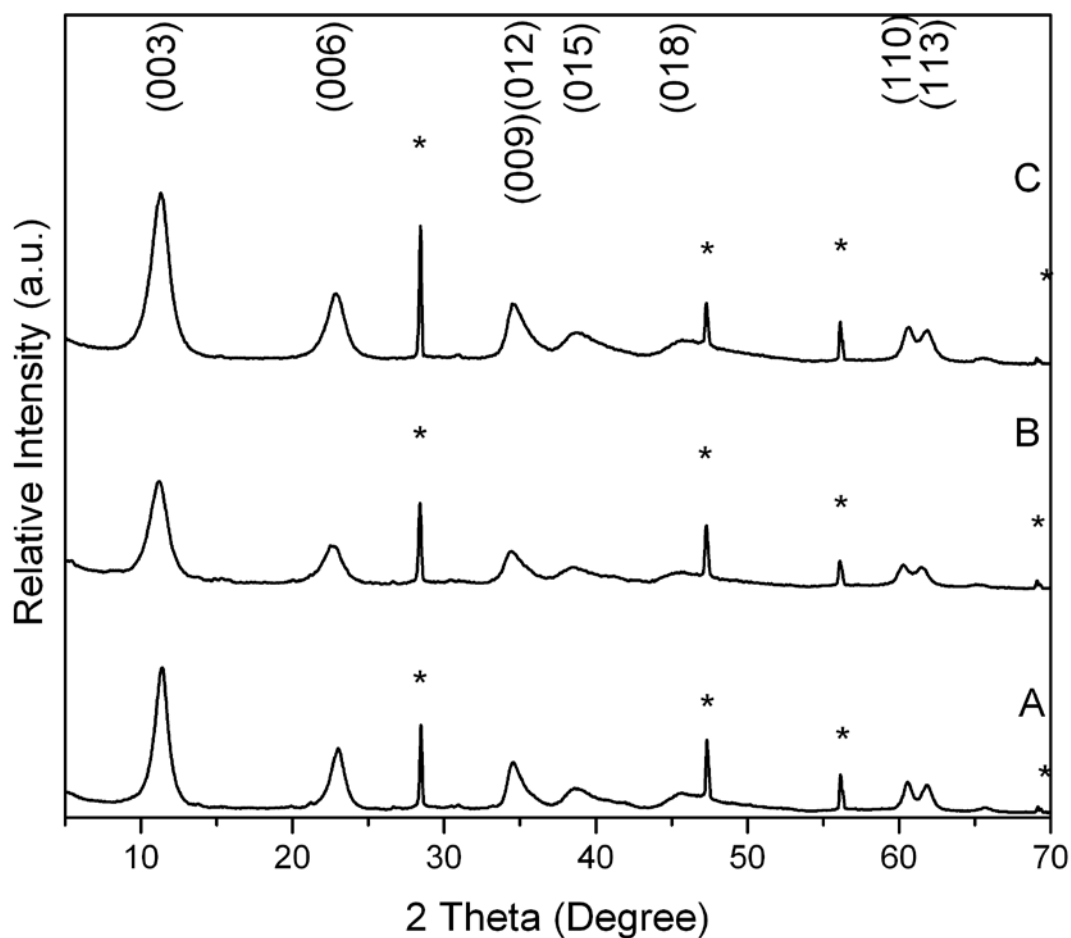


Figure 3. XRD patterns of layered double hydroxides synthesized by coprecipitation method with various cation compositions: A – Mg/Al; B- Co/Mg/Al; C- Ni/Mg/Al. Reflections from Si crystal used as a reference are marked with asterisk.

patterns (Figure 3.), the hydrotalcite type phase was identified in all synthesized layered double hydroxides.

More intense and sharper reflections of the (003) and (006) planes at low 2θ values (11-23°), and broad asymmetric reflections at higher 2θ values (34-66°) can be observed in the XRD patterns. The (009) reflection overlaps with the (012), resulting in a broad signal. Therefore, it can be concluded that it is possible to obtain hydrotalcite-like layered structures with the Co^{2+} or Ni^{2+} , Mg^{2+} and Al^{3+} cations in the chosen range of compositions. However, the intensities of some reflections for different LDH samples are slightly different, possibly indicating different degree of their crystallinity. Determined cell parameters c and a are shown in Table 1.

Table 1. Crystallographic data and crystallite size of synthesized layered double hydroxides.

| Sample | d_{003} | d_{006} | d_{110} | Cell parameters (Å) | | Crystallite size (Å) | |
|----------|-----------|-----------|-----------|---------------------|------|----------------------|-------|
| | (Å) | (Å) | (Å) | c | a | (003) | (110) |
| Mg/Al | 7.77 | 3.86 | 1.53 | 23.25 | 3.06 | 91 | 111 |
| Co/Mg/Al | 7.93 | 3.92 | 1.53 | 23.59 | 3.07 | 61 | 83 |
| Ni/Mg/Al | 7.87 | 3.89 | 1.53 | 23.40 | 3.05 | 64 | 85 |

The c parameter is related to the interlayer thickness, and is regulated by water content along with the amount, size, orientation, and charge of the anions located between the brucite-like layers. The cell parameter a is the average cation–cation distance inside the brucite-like layers [143]. The published interlayer distance of carbonate-containing Mg/Al LDH is 7.8 Å [130]. The d_{003} -values obtained for the synthesized LDH samples are very similar. Only a very low increase of the basal spacing is seen in the LDH samples containing cobalt and nickel. The calculated values of crystallite size of LDH samples are also

shown in Table 1. The dimensions in the a -direction are larger than that in the c -direction, as can be expected from the plate-like shape of hydrotalcite crystals [2]. Introduction of cobalt or nickel to the layered double hydroxides composition caused a considerable decrease in the crystallite size, which is in a good agreement with literature data [130]. The formation of smaller nano-sized primary crystallites could be a result of cobalt or nickel influence on the nucleation and crystal growth process during the precipitation of LDH. The compositions of the synthesized layered double hydroxides were analyzed by the X-ray fluorescence technique to determine differences of calculated and experimentally received compositions of materials (Table 2). The determined LDH molar compositions are very close to the nominal. However, the Al content is slightly lower than expected and this could be associated with partial solubility of aluminium ions as aluminate species under used synthesis conditions. LDH with cobalt has a lower content of Mg as was observed by S. Ribet [115]. The general formula for LDH indicates that it is possible to synthesize a number of compounds with different stoichiometries. In the natural hydrotalcites, the value of x is generally equal to 0.25. However, there are many difficulties in determining the exact value of x in LDH. Elemental analysis of the metal content in a solid phase will not give correct values if the LDH is not monophasic, *i.e.*, mixed with $M^{II}(OH)_2$, $M^{III}(OH)_3/M^{III}OOH$ or other phases which could segregate when the synthesis mixture contains either very high or very low M^{II}/M^{III} ratios. An intrinsic problem with these phases is their appearance as amorphous, which cannot be detected by XRD [3]. The obtained x values of synthesized LDH by XRF technique are in the expected range. They are not lower than 0.2 and not higher than 0.3. Thus, we can conclude from the results of XRF and XRD analyses that single-phase layered double hydroxides have formed during co-precipitation synthesis.

Table 2. Calculated and determined using XRF cation molar ratios in LDHs and formula of synthesized samples.

| Sample | $(M^y+Mg)/Al$ (molar ratio) | $M/(M+Mg)$ (at %) | Cations content in the LDH | | | Proposed formula ^z |
|----------|--------------------------------|----------------------|---|------|----------|---|
| | | | $[M^{II}_{1-x}M^{III}_x(OH)_2]^{x+}$ $(A^{m-})_{x/m}[nH_2O]$ | Mg | Co or Ni | |
| Mg/Al | 3.26 | | 0.77 | 0.23 | | $[Mg_{0.77}Al_{0.23}(OH)_2] (CO_3)_{0.115} H_2O$ |
| Co/Mg/Al | 2.86 | 16.85 | 0.62 | 0.12 | 0.26 | $[Mg_{0.62}Co_{0.12}Al_{0.26}(OH)_2] (CO_3)_{0.13} 0.91 H_2O$ |
| Ni/Mg/Al | 3.23 | 14.41 | 0.65 | 0.11 | 0.24 | $[Mg_{0.65}Ni_{0.11}Al_{0.24}(OH)_2] (CO_3)_{0.12} 1.14 H_2O$ |

^yM is cobalt or nickel respectively in Co/Mg/Al or Mg/Ni/Al samples.

^z Cations, adsorbed and interlayer water contents are measured, all others are calculated.

The carbonate content in synthesized samples was calculated from the M^{II}/M^{III} atomic ratios, assuming that carbonate is the only charge balancing interlayer anion. The water content in the formula was determined from the results of TG analyses which are presented below.

3.2. THERMAL DECOMPOSITION OF LDH

All layered double hydroxides undergo thermal decomposition at higher temperatures. Thermal gravimetric analysis of the natural hydrotalcite type sample Mg/Al and LDH with cobalt Co/Mg/Al and nickel Ni/Mg/Al was performed (Figs 4-6). The mass changes up to 200 °C are due to the removal of interlayer and adsorbed water [130]. Below this temperature dehydroxylation is minor and no decarbonation occurs. As seen from Figs 4-6, the endothermic processes of water removal continue until 250 °C and two DTG minima at 88 and 220 °C appear for all samples. The mass loss in this temperature interval was used for the calculation of water content (see Table 2). The decomposition of intralayer hydroxyl and carbonate anions occurs in the temperature range of 250-500 °C. The presence of a single mass loss in this range confirms the coupling of dehydroxylation and decarbonation processes. The presence of the transition metals in the synthesized LDH samples showed very minor effect on the thermal behavior of LDH. Therefore, the same temperature (650 °C) for thermal treatment of all samples was chosen.

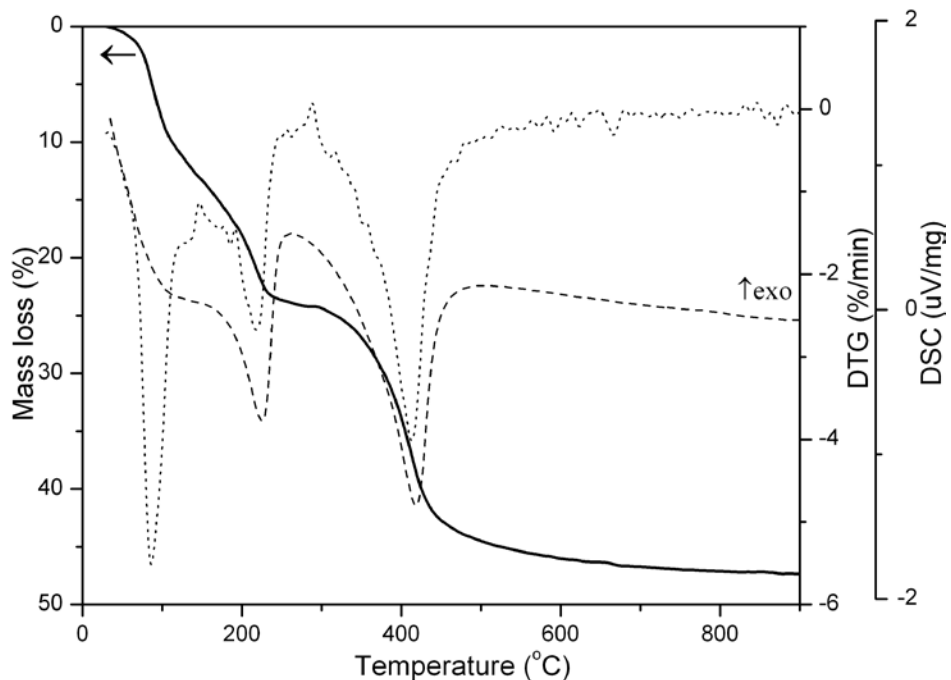


Figure 4. TG (solid line), DTG (dots line) and DSC (dashed line) curves of synthesized Mg/Al LDH.

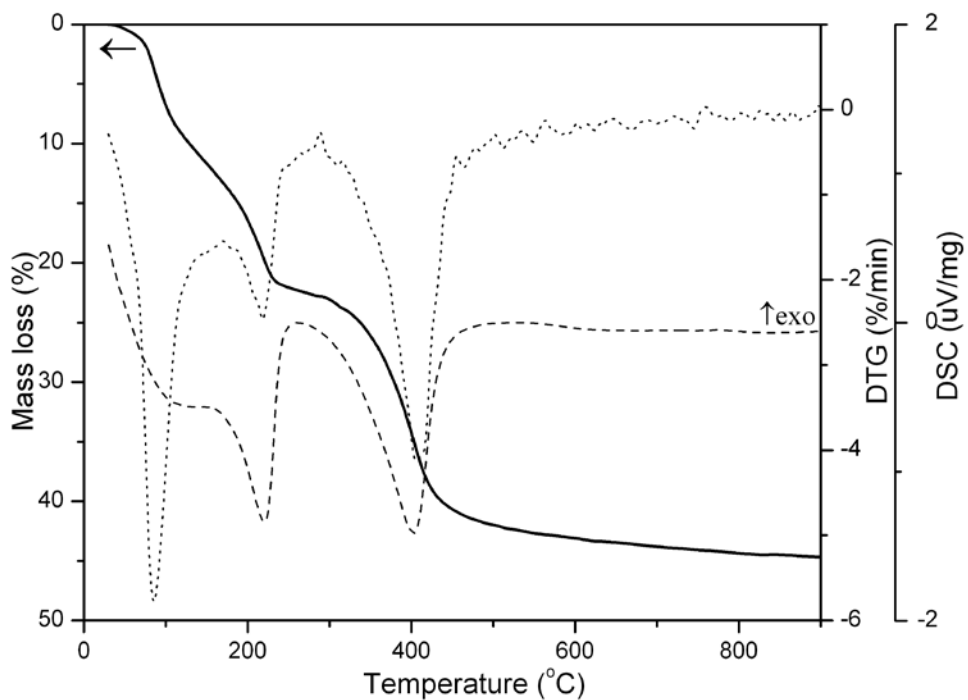


Figure 5. TG (solid line), DTG (dots line) and DSC (dashed line) curves of synthesized Co/Mg/Al LDH.

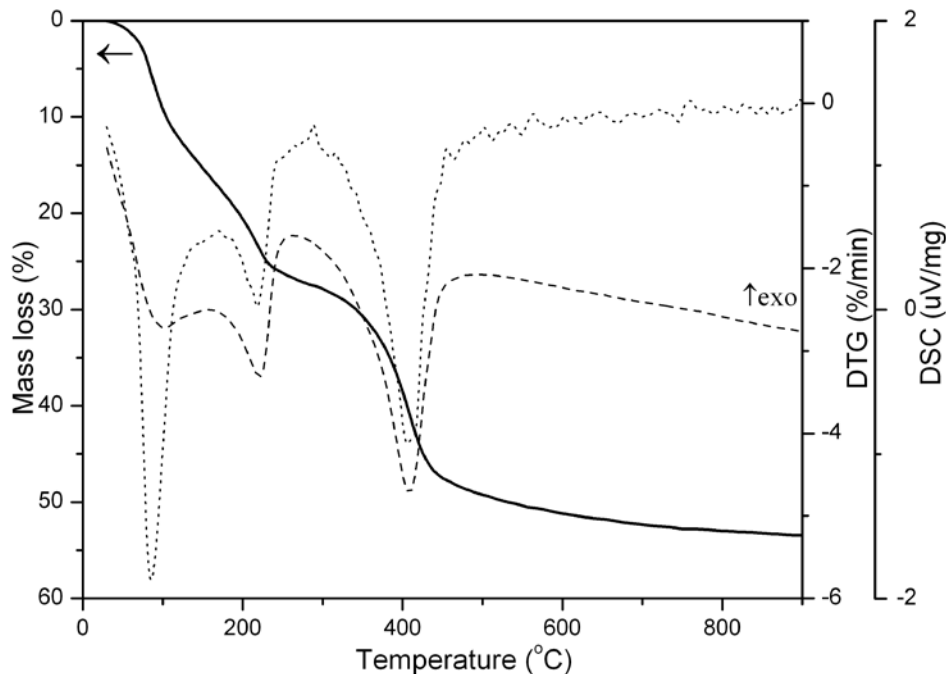


Figure 6. TG (solid line), DTG (dots line) and DSC (dashed line) curves of synthesized Ni/Mg/Al LDH.

The annealing temperature is very important because it is crucial for successful reconstitution of the layered structure. During the calcination of LDH, the temperature should be higher than the layer collapse but lower than the formation of spinel phase. This solid phase is stable and cannot be converted to LDH in water. Thus, for layered double hydroxides the calcinations temperature is usually set between 400 and 700 °C. The XRD analysis of heat-treated samples revealed the formation of poorly crystalline magnesium oxide (PDF # 75-1525) with peaks at $2\theta \approx 36, 43$ and 63° (Figure 7).

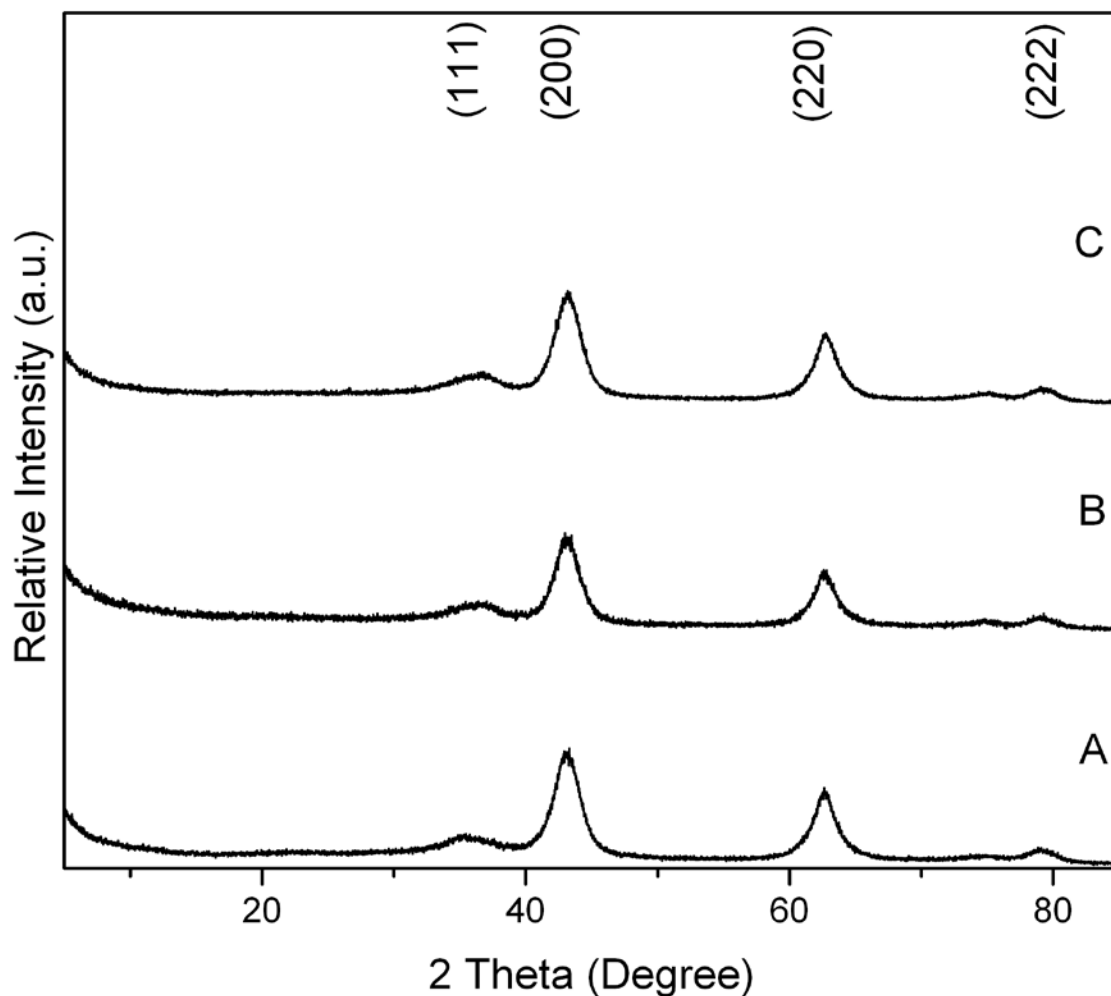


Figure 7. XRD patterns of mixed oxides after calcination of layered double hydroxides at 650 °C. A-Mg/Al₆₅, B- Co/Mg/Al₆₅, C- Ni/Mg/Al₆₅. Crystalline phase: MgO (PDF # 75- 1525).

These peaks are slightly shifted to higher 2θ angles in comparison with a pure magnesium oxide. This is a consequence of the incorporation of aluminium in the framework of the MgO, resulting in the formation of a mixed-metal oxide [13]. No peaks assigned to the transition metal oxides were observed. Moreover the XRD patterns of the samples Mg/Al₆₅, Co/Mg/Al₆₅, Ni/Mg/Al₆₅ do not show the formation of spinel-type crystalline phases. Consequently, these results clearly

show that the possibility to reform them to layered double hydroxides is very realistic.

3.3. REFORMATION OF LDH IN WATER

The chart of LDH behaviour during the cycle synthesis-thermal decomposition-regeneration is presented in Figure 8. The second part shows the reformation of calcined layered double hydroxides to a layered structure. Investigations of this process in water media at room and 80 °C temperature will be discussed in this section.

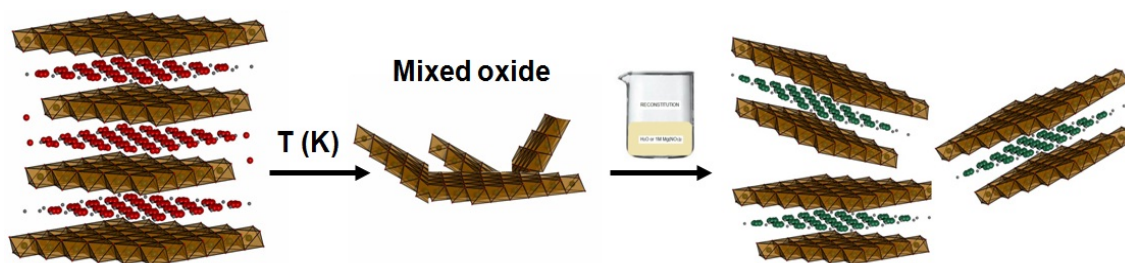


Figure 8. Chart of decomposition of synthesized layered double hydroxide and reformation of formed mixed metal oxides back to layered structure in aqueous media.

The XRD patterns of LDH samples obtained after the hydration process at room and 80 °C temperatures are given in Figure 9 and Figure 10 respectively. The reference patterns of Mg/Al hydrotalcite show regeneration of layered structure in water at both temperatures. The mixed-metal oxide transformed fully into LDH. However, the calcined LDHs with cobalt or nickel form more stable mixed-metal oxide phases, since incomplete regeneration was observed in water at room temperature. Interestingly, this oxide phase disappears with heat treatment of the reconstitution process, suggesting the high influence of the medium temperature on the reformation of layered double hydroxide. All reformed

samples exhibited the XRD patterns characteristic to the LDH structure (PDF # 22-700). Intense and narrow diffraction peaks at 11° and 22°, ascribed to (003) and (006) planes, respectively, are clearly seen.

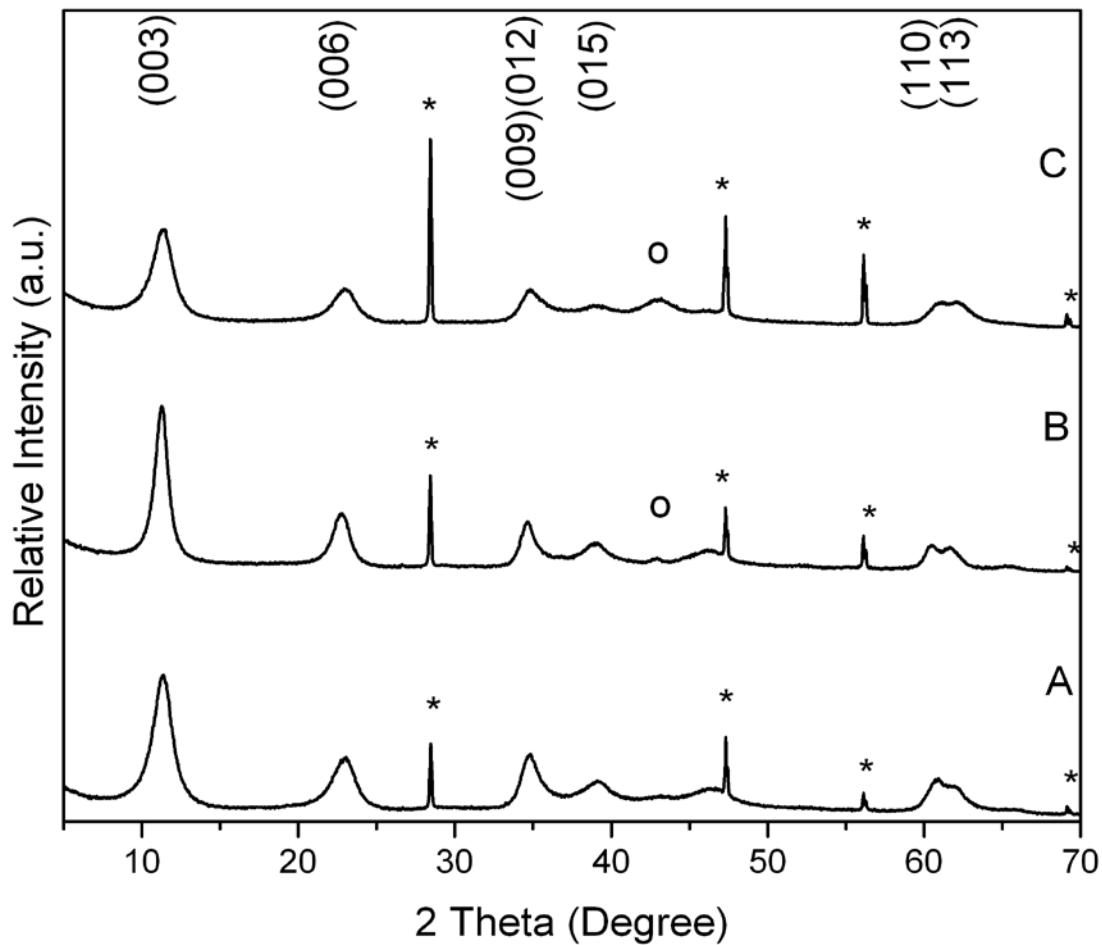


Figure 9. XRD patterns of reconstituted layered double hydroxides in water at 20 °C. (A- Mg/Al_{w20}; B- Co/ Mg/Al_{w20}; C- Ni/Mg/Al_{w20}). Side phases: O - MgO, * - Si.

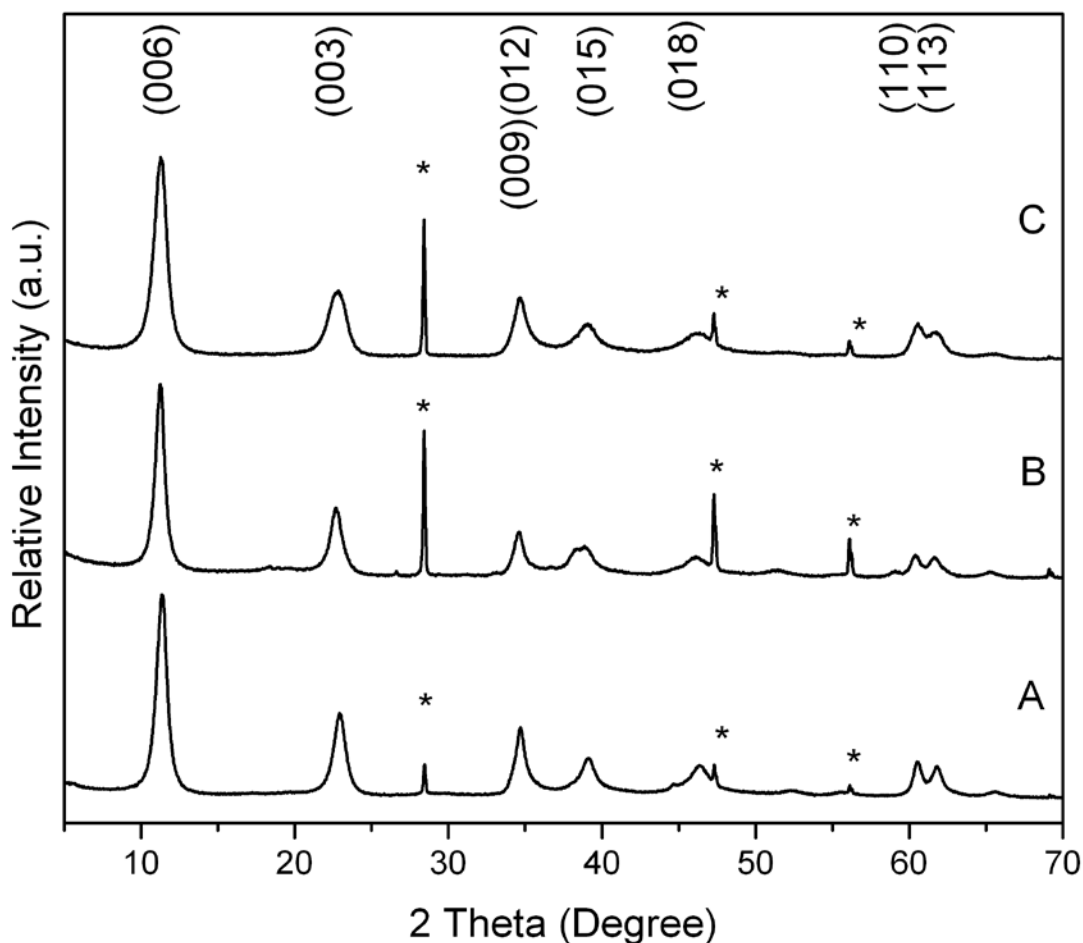


Figure 10. XRD patterns of reconstituted layered double hydroxides in water at 80 °C. (A- Mg/Al_{w80}; B- Co/ Mg/Al_{w80}; C- Ni/Mg/Al_{w80}). Phase: * - Si.

Wide and asymmetric (0kl) reflections were obtained above 30° 2θ values, as usually observed. The (110) and (113) reflections were noted around 61°. The peaks in Figure 9 (B and C) at 43° are attributed to remaining mixed metal oxides and indicate incomplete reconstitution of layered double hydroxide. The positions of the (003), (006) and (110) reflections allowed us to calculate the *c* and *a* cell parameters of reconstituted LDH, assuming the hexagonal lattice. The data are reported in Table 3. The lattice parameters for all samples are almost identical to their initial lattice parameters of as synthesized samples (see Table 1.), although variations were expected due to substitution of carbonate by OH⁻ ions. The

presence of carbonates in reformed samples can be due to the dissolved CO₂ in water. Contrary to the Mg/Al-containing samples, the samples containing transition metals show negligible decrease in the basal spacing after reconstitution in water.

Table 3. Crystallographic data and crystallite size of formed LDH after reformation in water.

| Sample | Temperature of water (°C) | d_{003} (Å) | d_{006} (Å) | d_{110} (Å) | Cell parameters | | Crystallite size (003) (Å) |
|-------------------------|---------------------------|------------------|------------------|------------------|-----------------|---------|-------------------------------|
| | | | | | c (Å) | a (Å) | |
| Mg/Al _{w20} | 20 | 7.79 | 3.86 | 1.52 | 23.28 | 3.05 | 62 |
| Mg/Al _{w80} | 80 | 7.81 | 3.88 | 1.53 | 23.34 | 3.06 | 117 |
| Co/Mg/Al _{w20} | 20 | 7.88 | 3.90 | 1.53 | 23.52 | 3.06 | 91 |
| Co/Mg/Al _{w80} | 80 | 7.89 | 3.91 | 1.53 | 23.57 | 3.06 | 131 |
| Ni/Mg/Al _{w20} | 20 | 7.82 | 3.86 | 1.52 | 23.31 | 3.04 | 58 |
| Ni/Mg/Al _{w80} | 80 | 7.84 | 3.89 | 1.53 | 23.44 | 3.06 | 94 |

It is known that changes of the parameter a , that is sensitive to the ionic radii of the layer cations, could be associated to the extraction of Al³⁺ from the brucite layer [144]. In this study, the parameter a in synthesized and reformed samples is almost equal even when the samples were not fully reformed. These results show that extraction of cations other than Al³⁺ from the layers has negligible effect on the cell parameter a . Figure 10 presents the XRD patterns of reconstructed LDH at 80 °C. Evidently, full reformation of layered structure occurs. Besides the diffraction peaks are sharper compared to the same peaks of samples reformed at lower temperature. The slightly different intensities, perhaps, indicate different degree of sample crystallinity. The calculated values of crystallite size of reformed

LDH samples are also shown in Table 3. The obtained values are compared to as synthesized samples in Figure 11.

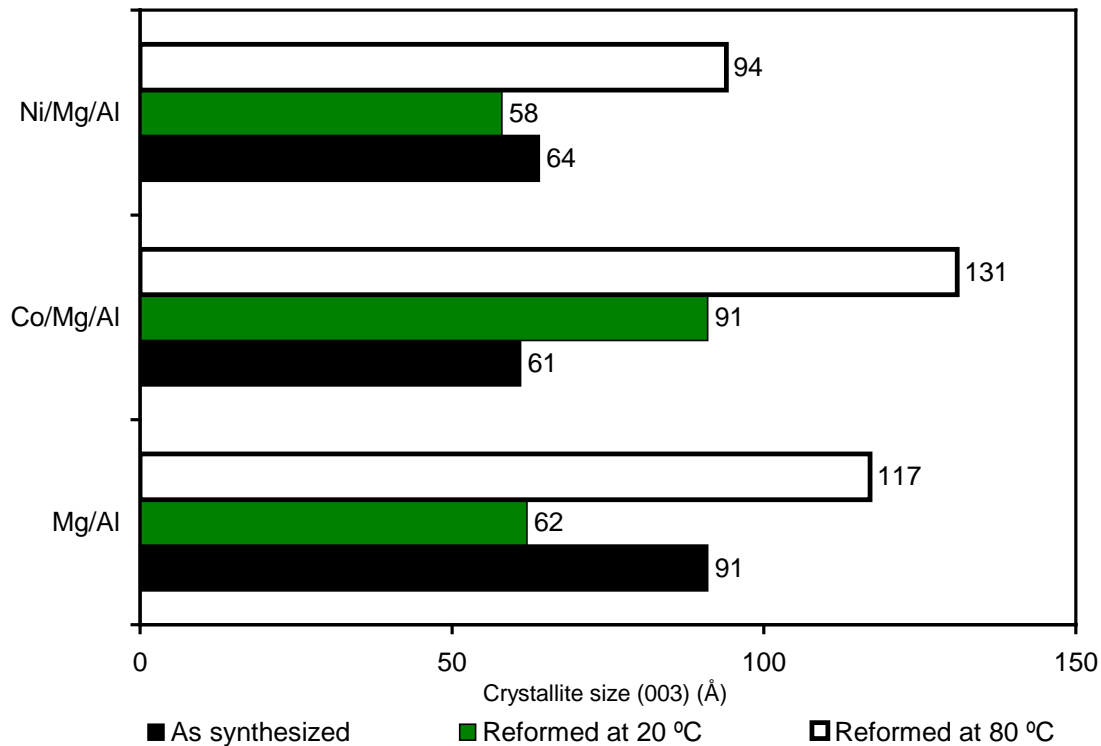


Figure 11. Crystallite size of as synthesized and reformed in water layered double hydroxides.

The results presented in Figure 11 show that the temperature of reformation media has a strong influence on crystallite size of LDH. After increasing the medium temperature up to 80 °C, for Mg/Al LDH the crystallite size increases from 91 to 117 Å (29 %), for Co/Mg/Al from 61 to 131 Å (115 %) and for Ni/Mg/Al LDH from 64 to 94 Å (47%). Thus, we can conclude that the increase of reformation temperature gives an opportunity for a full recovery of the layered structure even for transition metal containing LDHs and also affects the crystallinity of reconstituted LDH.

Only a few recent studies have analyzed the influence of a third metal cation, such as Ni^{2+} , on the memory effect of calcined Mg/Al hydrotalcite [130]. In our case it can be concluded, that calcined LDH exposed to water show reconstruction, but the presence of nickel or cobalt in the sample reduces the ability of LDH to recover the original layered structure. The different reformation behaviour of the binary Mg/Al and the ternary Ni/Mg/Al or Co/Mg/Al samples suggests the intimate association of both divalent metals in the mixed oxide phase. Very interesting results were observed after reformation at higher temperature (80 °C). Mixed metal oxide phase disappears and only layered double hydroxide phase can be observed in the XRD patterns. Thus, the high temperature of reconstitution media enables full reformation of layered structure in contrast to other studies [119, 130]. The results of *in situ* EDXRD and modeling of kinetics using the Avrami-Erofe'ev expression showed that the reconstitution reaction occurs by dissolution of mixed oxide followed by crystallization of the LDH from solution [85]. At room temperature, the rate of crystallization is dependent on the rate of formation of nucleation sites for crystal growth, whereas the rate of crystal growth at the surface of these nucleation sites and the rate of transport of reactive material to these sites has a minor influence on the overall rate. As the temperature is increased, the rate of formation of nucleation site increases and the reaction only depends on the rate at which reactive material reaches the already-formed sites, i.e. the reaction becomes diffusion-limited in the second stage. With addition of third metal to binary system the inhibiting effect occurs at low temperature and not full dissolution of mixed oxides phase is observed. From our results the positive influence of temperature on the reformation is evident. To justify dissolution-crystallization mechanism during the memory effect of LDH, the influence of different reformation solutions will be discussed in the next section.

3.4. REFORMATION OF LDH IN $Mg(NO_3)_2$ SOLUTION

The dissolution-crystallization mechanism of mixed oxide regeneration well explains the formation of LDH with new anions and implies a possibility for changing the cation composition of LDH during regeneration process. To our knowledge, for the first time, the reformation in magnesium nitrate media was performed. The XRD patterns of mixed oxides after treatment in $Mg(NO_3)_2$ solution at room temperature and 80 °C are given in Figures 12 and 13 respectively.

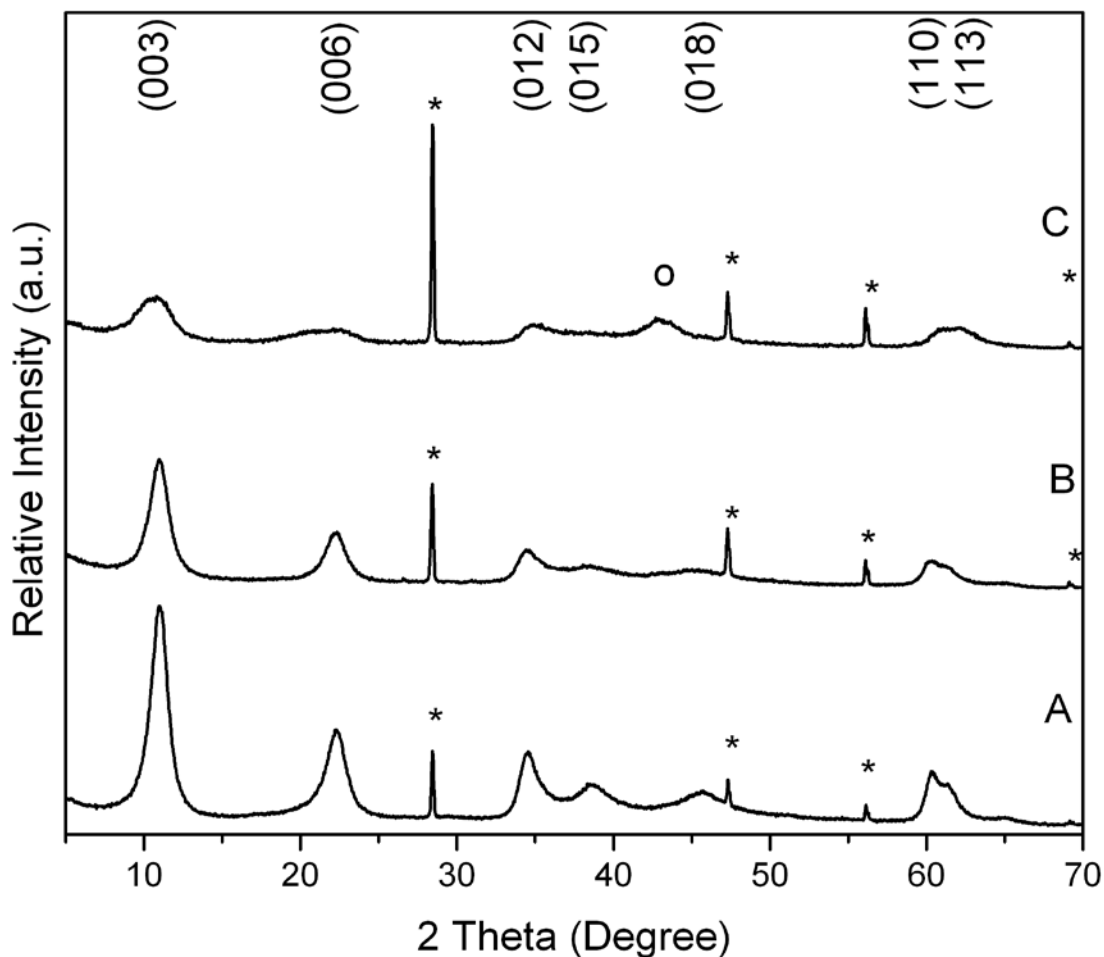


Figure 12. XRD patterns of reconstituted layered double hydroxides in $Mg(NO_3)_2$ solution at 20 °C. (A- Mg/Al_{N20} ; B- $Co/Mg/Al_{N20}$; C- $Ni/Mg/Al_{N20}$). Side phases: O - MgO , * - Si .

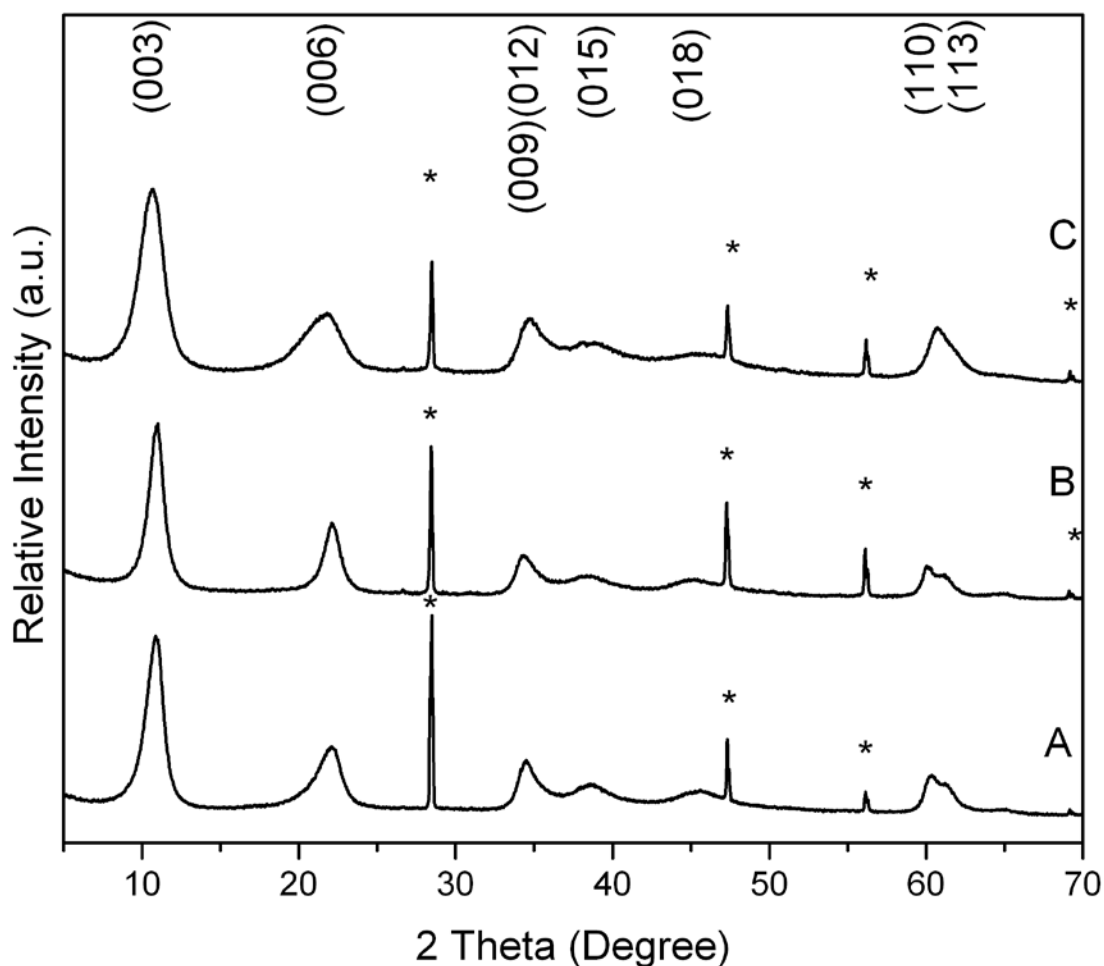


Figure 13. XRD patterns of reconstituted layered double hydroxides in $\text{Mg}(\text{NO}_3)_2$ solution at 80 °C. (A- $\text{Mg}/\text{Al}_{\text{N80}}$; B- $\text{Co}/\text{Mg}/\text{Al}_{\text{N80}}$; C- $\text{Ni}/\text{Mg}/\text{Al}_{\text{N80}}$). Side phase: * - Si.

The XRD patterns of all samples show the characteristic XRD pattern of the LDH (PDF # 22-700). However, the reformation of $\text{Ni}/\text{Mg}/\text{Al}$ LDH at room temperature does not proceed fully. The minor amount of oxide phase is present in the sample. Interestingly, the XRD patterns of LDHs reconstituted in magnesium nitrate solution are slightly different in comparison with those of as synthesized (Figure 3) and reformed in water (Figures 9-10) samples. The 003 peak is shifted to a lower 2θ angle for all three samples, indicating that the interlayer region is expanded by the intercalation of a larger anion, which is most likely nitrate.

Obvious decrease of intensity and sharpness of diffraction peaks can be also observed. The reformation in the magnesium nitrate solution has the strongest effect on the c parameter of LDH (Table 4). The basal spacing represents the thickness of a single layer and is normally related to the size of charge balancing interlayer anions. For the samples reformed in the magnesium nitrate solution, the basal spacings d_{003} are higher than 8 Å. This corresponds to the values of basal spacing of nitrate containing LDH [145]. Following the evolution of the parameter c (or better the interlayer free distance, determined as $IFD = c - 4.8$ (Å), where 4.8 Å is the thickness of the brucite layer) it can be observed that samples reformed at 80 °C display higher IFD values compared to the analogous samples reformed at room temperature. Therefore, a higher amount of nitrate anions could be expected in the composition of LDH. The crystallite dimensions for LDH samples were also evaluated and presented in Table 4.

Table 4. Crystallographic data and crystallite size of formed LDH after reformation in magnesium nitrate solution.

| Sample | Temperature of reconstitution. (°C) | d_{003} (Å) | d_{006} (Å) | d_{110} (Å) | Cell parameters | | Crystallite size (003) (Å) |
|-------------------------|--|------------------|------------------|------------------|-----------------|---------|-------------------------------|
| | | | | | c (Å) | a (Å) | |
| Mg/Al _{N20} | 20 | 8.03 | 3.98 | 1.53 | 23.99 | 3.07 | 70 |
| Mg/Al _{N80} | 80 | 8.20 | 4.02 | 1.53 | 24.36 | 3.07 | 69 |
| Co/Mg/Al _{N20} | 20 | 8.08 | 3.99 | 1.53 | 24.10 | 3.07 | 61 |
| Co/Mg/Al _{N80} | 80 | 8.12 | 4.01 | 1.54 | 24.22 | 3.08 | 80 |
| Ni/Mg/Al _{N20} | 20 | 8.11 | 3.93 | 1.52 | 23.97 | 3.04 | 28 |
| Ni/Mg/Al _{N80} | 80 | 8.27 | 4.05 | 1.52 | 24.57 | 3.05 | 47 |

The obtained values are compared to those of as synthesized samples in Figure 14. Evidently, the crystallite size of LDH depends on the reconstitution media, temperature and chemical composition of regenerated LDH. However, the reason for wide distribution of crystallite size at different conditions is still unclear.

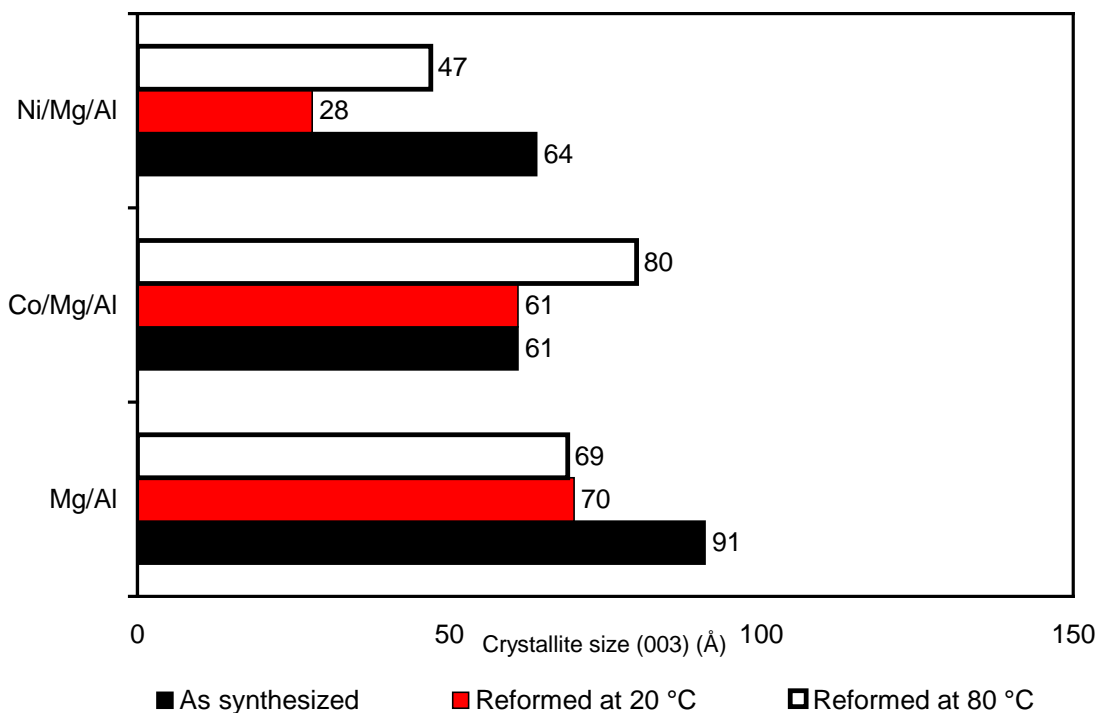


Figure 14. Crystallite size of layered double hydroxides as synthesized and reformed in magnesium nitrate solution.

The composition of reformed LDH cations in magnesium nitrate solution at room temperature was studied by XRF. The results are presented in Table 5. All samples after treatment in magnesium nitrate have a higher concentration of magnesium. The small increase in the M^{II}/M^{III} ratio (3.26 and 3.71 for Mg/Al and Mg/Al_{N20} respectively; 3.23 and 3.34 for Ni/Mg/Al and Ni/Mg/Al_{N20}, respectively) was also observed.

Table 5. The calculated and obtained by XRF measurement molar ratios of cations in LDH and formula of samples reconstituted in $\text{Mg}(\text{NO}_{3/2})_2$ solution at 20 °C.

| Sample | $(\text{M}^y + \text{Mg}) / \text{Al}$ (molar ratio) | $\text{M} / (\text{M} + \text{Mg})$ (at %) | Cations content in the | | | Proposed formula |
|--|---|---|---|------|----------|--|
| | | | LDH | Mg | Co or Ni | |
| $\text{Mg}/\text{Al}_{\text{N}20}$ | 3.71 | | $[\text{M}^{\text{II}}_{1-x} \text{M}^{\text{III}}_x (\text{OH})_2]^{\text{x}+}$ $(\text{A}^{\text{m-}})_{\text{x}/\text{m}}] \text{nH}_2\text{O}$ | 0.79 | 0.21 | $[\text{Mg}_{0.79} \text{Al}_{0.21} (\text{OH})_2] (\text{A}^{\text{m-}})_{0.21/\text{m}}] \text{nH}_2\text{O}$ |
| $\text{Co}/\text{Mg}/\text{Al}_{\text{N}20}$ | 3.71 | 13.32 | | 0.68 | 0.11 | $[\text{Mg}_{0.68} \text{Co}_{0.11} \text{Al}_{0.21} (\text{OH})_2] (\text{A}^{\text{m-}})_{0.21/\text{m}}] \text{nH}_2\text{O}$ |
| $\text{Ni}/\text{Mg}/\text{Al}_{\text{N}20}$ | 3.34 | 14.35 | | 0.66 | 0.11 | $[\text{Mg}_{0.66} \text{Ni}_{0.11} \text{Al}_{0.23} (\text{OH})_2] (\text{A}^{\text{m-}})_{0.23/\text{m}}] \text{nH}_2\text{O}$ |

^yM is cobalt or nickel respectively in $\text{Co}/\text{Mg}/\text{Al}_{\text{N}20}$ or $\text{Mg}/\text{Ni}/\text{Al}_{\text{N}20}$ samples.

Therefore, after regeneration the most affected samples are the LDHs containing cobalt, where the M^{II}/M^{III} ratio increases from 2.86 in the Co/Mg/Al sample to 3.71 in Co/Mg/Al_{N20} sample. Apparently, the lower amount of cobalt calculated in the Co/Mg/Al_{N20} is associated with increase of magnesium content in composition. It is important to note that no loss of the transition metal was detected.

From these results we can confirm that the reconstitution is a process of dissolution of mixed-metal oxide and subsequent crystallization of layered double hydroxide. This explains well the formation of LDHs with new anions and implies a possibility for changing of the cation composition.

3.5. INFLUENCE OF REFORMATION ON MORPHOLOGY

The influence of reformation process on the surface morphology of the LDH samples was investigated using SEM. The SEM micrographs of representative nickel containing LDHs are presented in Figures 15-17. It can be seen from Figure 15, that as-synthesized Ni/Mg/Al LDH is composed of large (1-3 μm) flat plate-like crystallites. The surface of regenerated Ni/Mg/Al_{W20} contains agglomerated particles ($\sim 10 \mu\text{m}$) which are covered by smaller (1-3 μm) crystallites (see Figure 16). Figure 17 shows the SEM micrograph of reformed Ni/Mg/Al_{N20} LDH sample in magnesium nitrate. As seen, many small particles ($\sim 1 \mu\text{m}$) are partially aggregated. In some areas aggregates of fibrous particles can also be found. In conclusion, the morphology of regenerated Ni/Mg/Al_{W20} and Ni/Mg/Al_{N20} LDH samples is slightly different in comparison with as-synthesized Ni/Mg/Al sample. The LDH samples after reformation consist of large particles with sharp edges along with a high number of smaller particles.

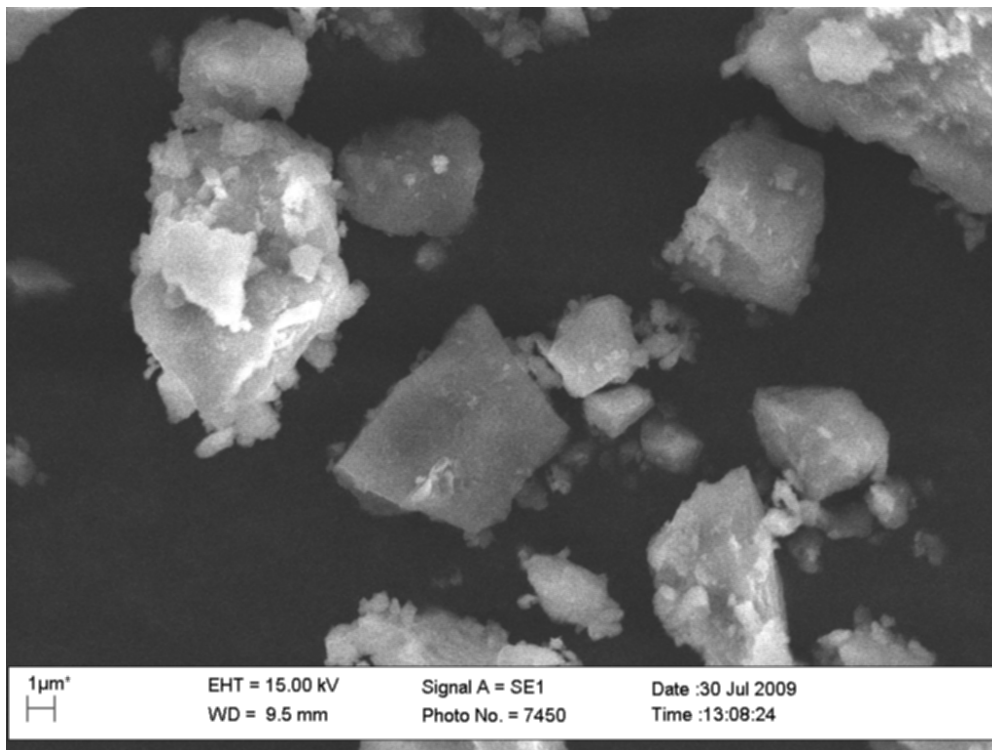


Figure 15. SEM micrograph of as-synthesized Ni/Mg/Al LDH.

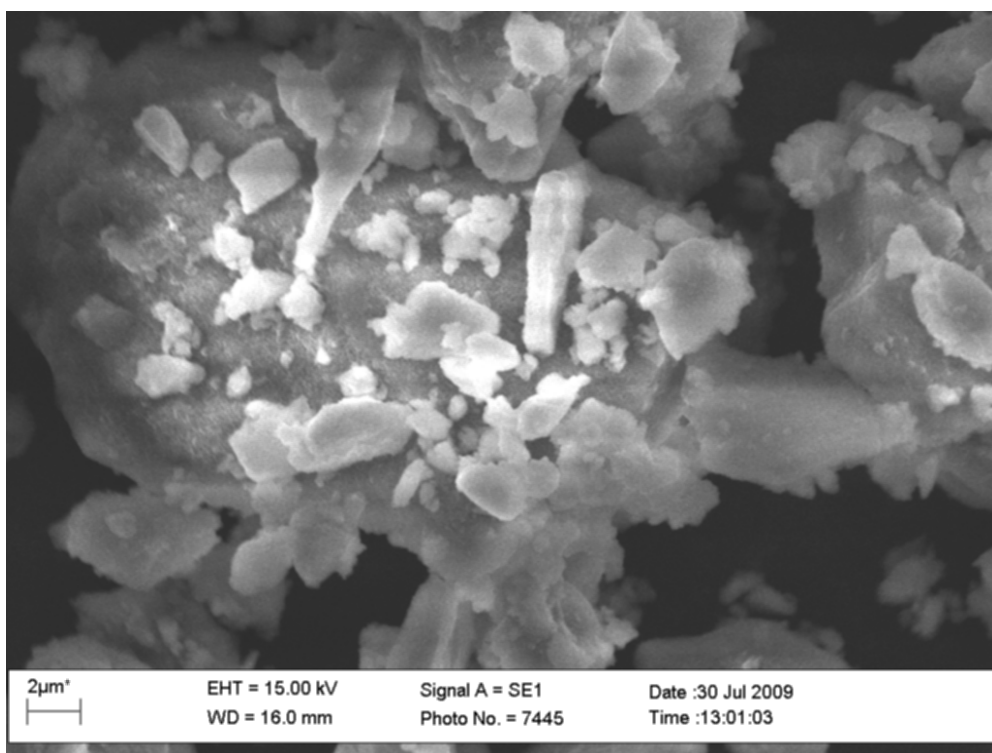


Figure 16. SEM micrograph of Ni/Mg/Al_{w20} LDH after hydration in water.

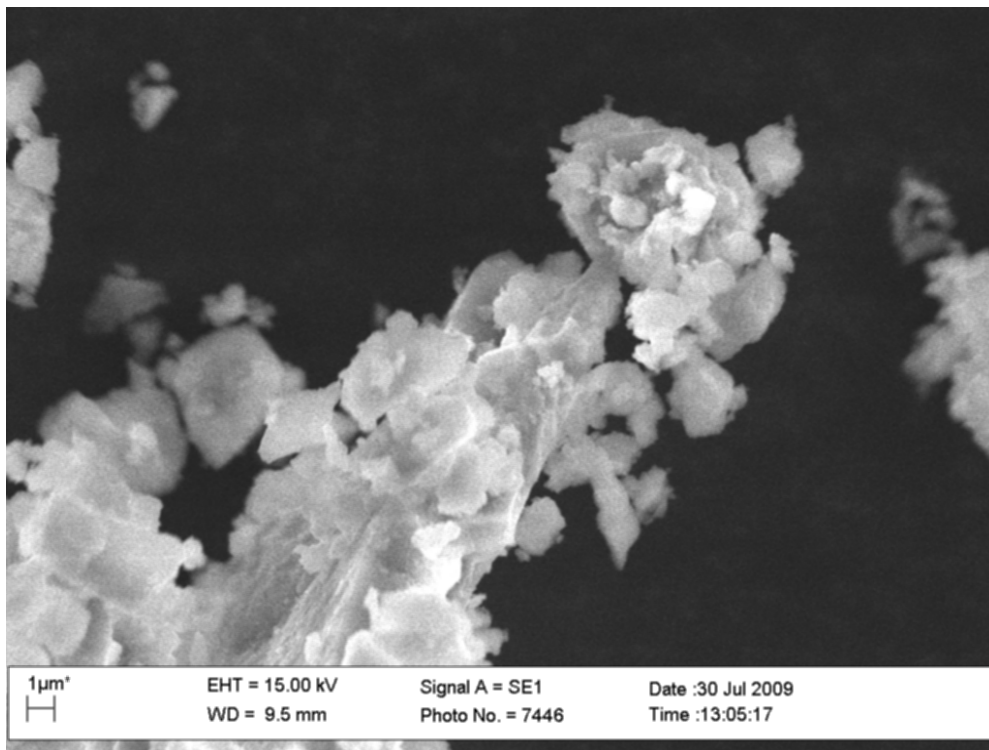


Figure 17. SEM micrograph of Ni/Mg/Al_{N20} LDH after regeneration in the magnesium nitrate solution.

Very important characteristic of layered double hydroxides is the formation of high specific surface area after thermal treatment. The adsorption of N₂ gas is often used to evaluate the surface-accessible area and pore size distribution by the Brunauer–Emmett–Teller (BET) and Barret- Joyner- Halenda (BJH) methods. The accessible surface is generally that of the internal pores within the crystallites and the external surface between the crystallites. Correspondingly, the measured pores are those inside and between the crystallites. The influence of reformation process on the specific surface area and pore size of mixed metal oxides were investigated and the results are presented in Table 6.

Table 6. Surface areas, pore volumes and pore diameters of calcined LDH.

| Samples calcined at 650 °C | Outgas temp. °C | Surface area (BET) m ² g ⁻¹ | Total pore volume cm ³ g ⁻¹ | Average pore diameter Å | Max. pore diameter Å |
|-------------------------------|--------------------|--|--|----------------------------|-------------------------|
| Co/Mg/Al ₆₅ | 250 | 169.73 | 0.365 | 85.95 | 62.30 |
| Co/Mg/Al _{W20} | 250 | 94.22 | 0.303 | 128.60 | 100.10 |
| Co/Mg/Al _{W80} | 250 | 130.70 | 0.334 | 102.30 | 74.10 |
| Co/Mg/Al _{N20} | 250 | 110.50 | 0.342 | 123.90 | 18.6-99.4 |
| Co/Mg/Al _{N80} | 250 | 145.40 | 0.372 | 102.50 | 74.00 |
| | | | | | |
| Ni/Mg/Al ₆₅ | 400 | 199.40 | 0.315 | 63.22 | 56.24 |
| Ni/Mg/Al _{W20} | 400 | 189.94 | 0.311 | 65.39 | 61.74 |
| Ni/Mg/Al _{W80} | 400 | 195.86 | 0.319 | 65.05 | 60.32 |
| Ni/Mg/Al _{N20} | 400 | 178.52 | 0.245 | 54.89 | 49.88 |
| Ni/Mg/Al _{N80} | 400 | 175.02 | 0.271 | 61.89 | 50.03 |

The N₂ adsorption isotherms (desorption isotherms are not shown) of the nickel or cobalt containing LDH exhibited type IV isotherms which are characteristic for mesoporous materials. The isotherms exhibit slight adsorption at low relative pressure due to the presence of micropores. An increase at high relative pressure indicates interparticle porosity, which seems to show that formed mixed oxides consist mainly of non-porous nanoparticles within the nanometer range (Figures 18 and 19). It has been reported that the decomposition of hydrotalcites preserves the overall particle shape and that the surface perpendicular to the basal planes appears cratered [146]. Moreover, materials of high surface area were obtained upon decomposition of LDH, irrespective of the starting material [127]. In this study LDHs with transition metals after calcination at 650 °C have high surface areas. For example Ni/Mg/Al₆₅ sample reaches almost 200 m²g⁻¹. The specific surface areas of cobalt containing samples decreased significantly upon

calcination of reformed LDH (from $170 \text{ m}^2\text{g}^{-1}$ for Co/Mg/Al₆₅ to $94 \text{ m}^2\text{g}^{-1}$ for Co/Mg/Al_{W20}). Introduction of cobalt in MgAlO mixed oxides lowers the surface areas [120]. The reformation in water and magnesium nitrate solution show the same negative effect on the specific surface areas. This could be explained by sintering features. The influence of reformation medium has different effect on the surface areas of mixed oxides with cobalt or nickel. Co/Mg/Al_{W20} and Co/Mg/Al_{W80} samples after calcination show lower values compared to calcined Co/Mg/Al_{N20} and Co/Mg/Al_{N80} samples. For the nickel containing samples the situation is completely reversed, the specific surface area of decomposed reconstituted Ni/Mg/Al₆₅ sample slightly decreases after treatment with nitrate solutions.

Porosity in calcined LDH is created by two different processes. The small intraparticle porosity occurs due to a “cratering” process. On the other hand, the irregular stacking of plate-like particles creates interparticle pores [33]. The size of these interparticle pores depends mainly on the crystal size; interparticle porosity contributes largely to the total pore volume (Table 6.). The pore size distribution graphics for all samples show one main peak that appears between 50-130 Å except Co/Mg/Al_{N20}. Figure 20 show the pore size distribution graphic of representative calcined Co/Mg/Al₆₅ sample. The mixed oxide samples containing cobalt show decrease in total pore volume and increase of average pore diameter compared to Co/Mg/Al₆₅ sample.

The chosen process to form mixed oxides (synthesis of LDH – calcination-reformation to LDH and again calcination) shows minor effect on pore dimensions. It can be concluded that reformation media has considerable influence on the morphology of mixed metal oxides. The effects for nickel or cobalt containing samples are different.

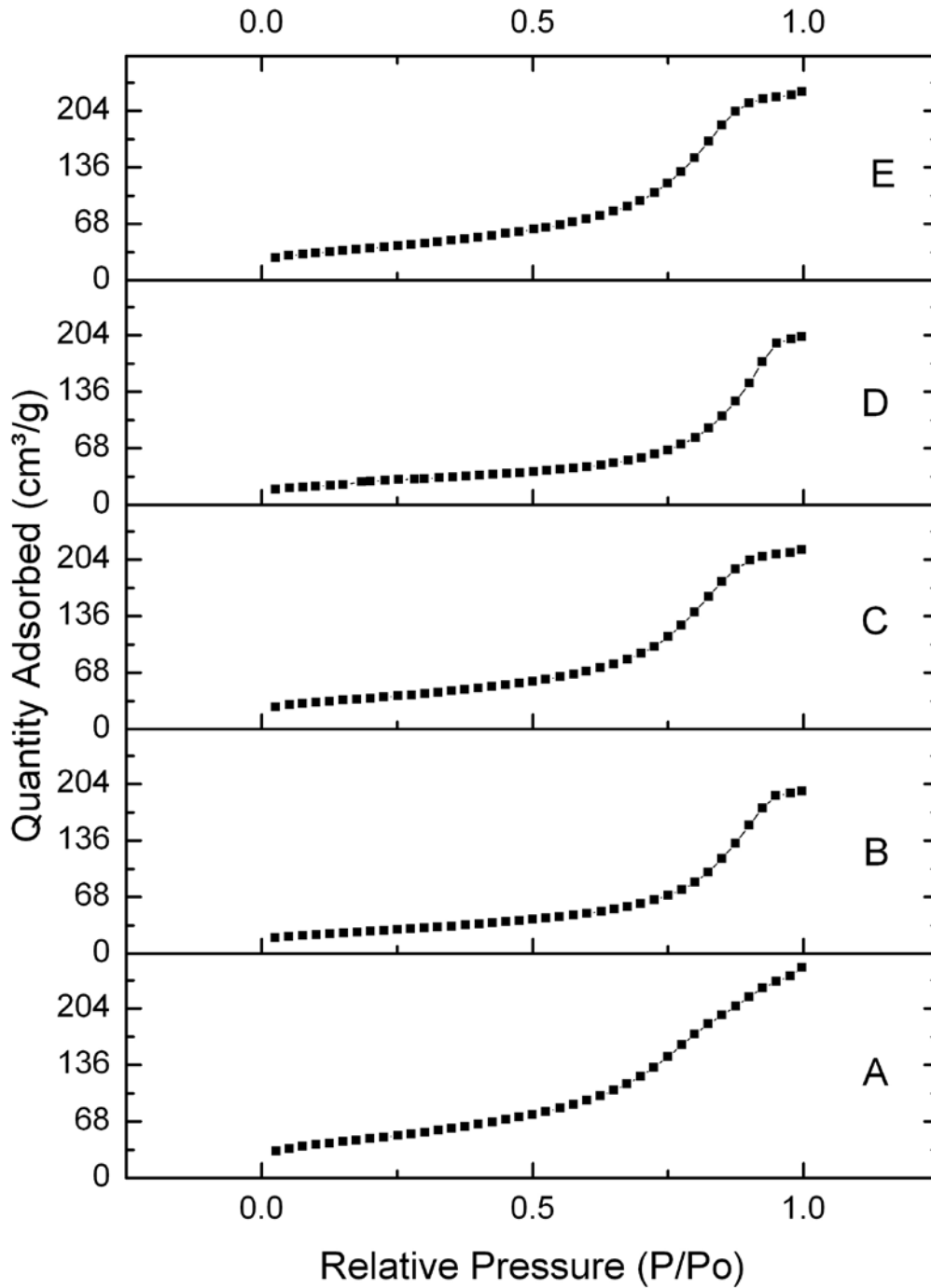


Figure 18. Adsorption isotherms linear plots for sample Co/Mg/Al₆₅ (A) and thermally treated at 650 °C samples Co/Mg/Al_{w20} (B); Co/Mg/Al_{w80} (C); Co/Mg/Al_{N20} (D); Co/Mg/Al_{N80} (E).

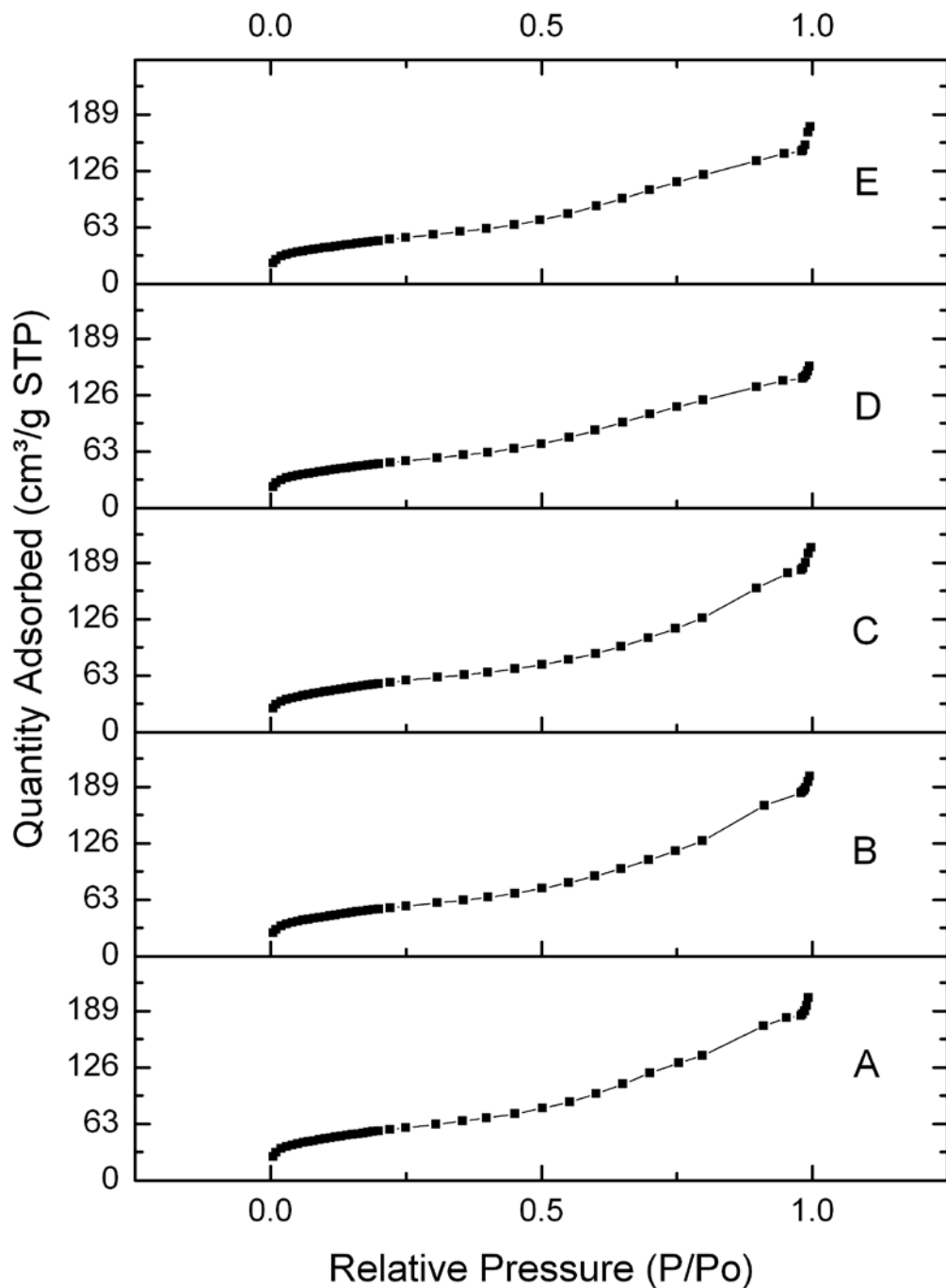


Figure 19. Adsorption isotherms linear plots for sample Ni/Mg/Al₆₅ (A) and thermally treated at 650 °C samples Ni/Mg/Al_{w20} (B); Ni/Mg/Al_{w80} (C); Ni/Mg/Al_{N20} (D); Ni/Mg/Al_{N80} (E).

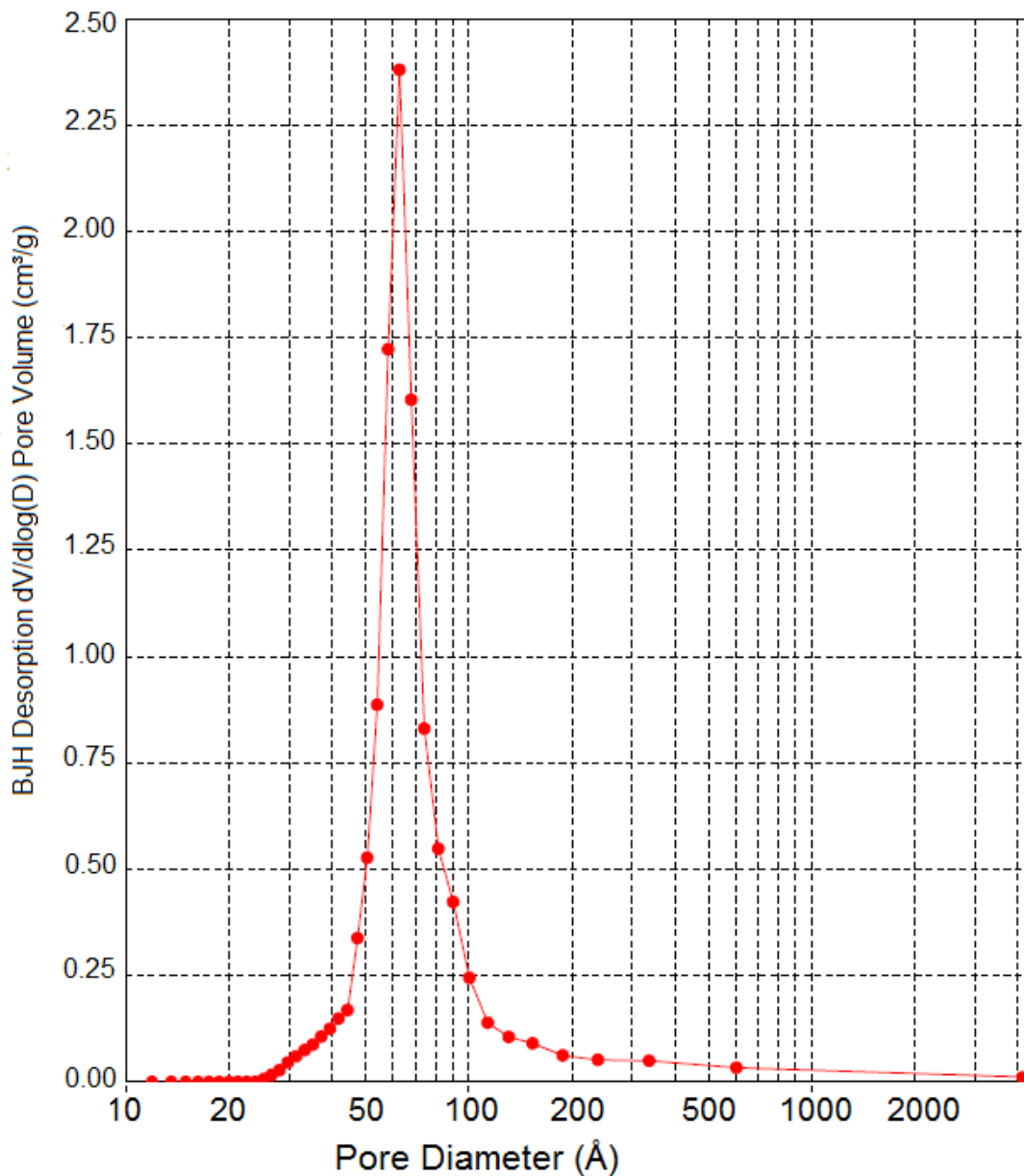


Figure 20. Pore size distribution from the N₂ desorption isotherm of the sample Co/Mg/Al₆₅.

3.6. APPLICATION OF REFORMED LDH

The field of gas purification was chosen to demonstrate how “memory effect” of layered double hydroxide can influence their catalytic activity. The activity for

the NO_x removal of the catalyst, based on mixed oxides, derived from cobalt containing LDH was compared. Hydrotalcites with cobalt in their structure have been described as active catalysts for the SO_x, NO and N₂O removal [14]. The possibility of using hydrotalcite derived materials as NO_x storage/reduction catalysts has also been studied [13]. In this work two cobalt containing LDH samples were analyzed in order to show how the reformation of mixed oxides derived from LDH can influence the activity of NO_x removal. Different reaction conditions: lean (530 ppm of NO, 50 ppm of C₃H₈, 13 % O₂) and rich (530 ppm of NO, 700 ppm of C₃H₈, 8 % O₂) were used.

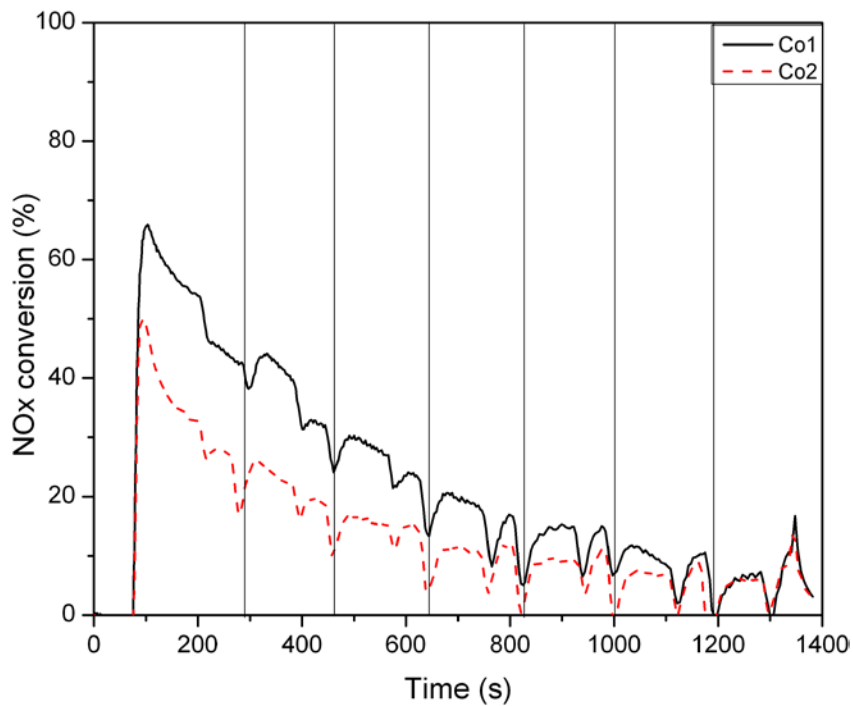


Figure 21. NO_x conversion during seven cycles lean – rich (120 s lean – 60 s rich) at 150 °C.

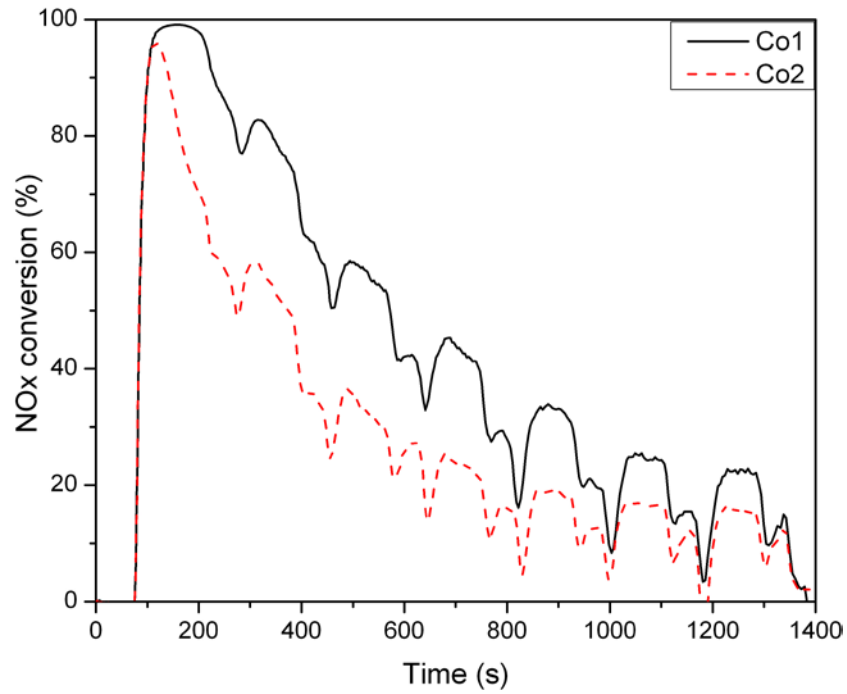


Figure 22. NO_x conversion during seven cycles lean – rich (120 s lean – 60 s rich) at 300 °C.

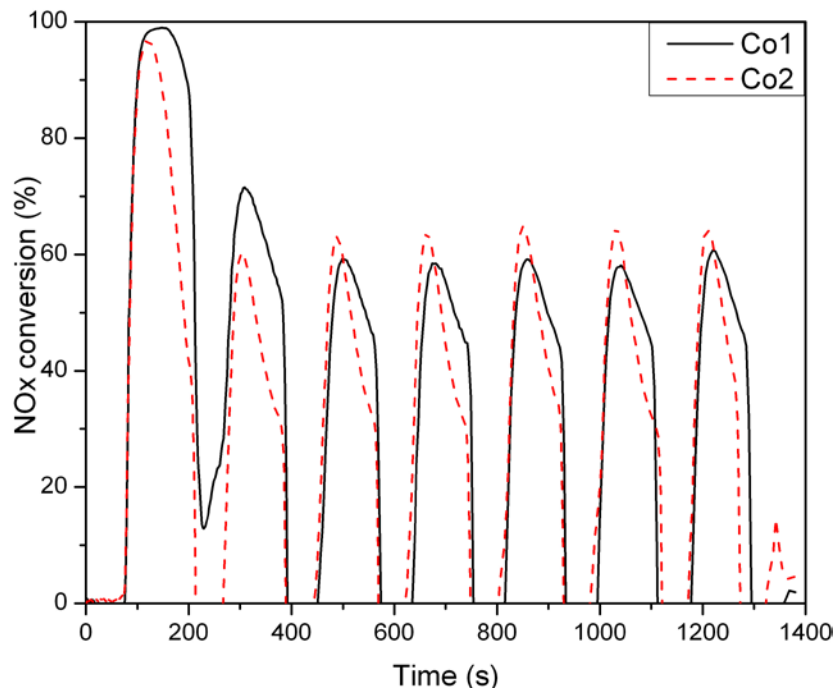


Figure 23. NO_x conversion during seven cycles lean – rich (120 s lean – 60 s rich) at 450 °C.

The NO_x conversion of seven lean - rich cycles, obtained with the reformed Co1 sample and just calcined Co2 sample, were compared at different temperatures and the results are shown in Figures 21-23. As can be seen, even without the presence of a noble metal, the catalysts present some activity for the NO_x removal at 150 °C. The most interesting result is that the Co1 sample shows higher activity at 150 and 300 °C temperatures as compared to the sample that was fresh calcined at 650 °C. The NO_x is efficiently removed during the first lean period, adsorbing the NO_x as nitrates, but the activity falls during the rich period, without recovering the initial activity in the successive cycles even at 450 °C temperature. Catalysts based on Co/Mg/Al mixed oxides from LDH precursors may be considered as promising materials for deNO_x catalysts, although the chemical composition and morphology have to be finely tuned. In the absence of cobalt there is no activity for the reduction of NO_x. The activity is related to the presence of cobalt centers. It has been shown, that only reduced forms of the transition metal show activity [14]. The catalytic results of Co1 and Co2 samples seem to indicate that reformation of LDH has influence to the final catalyst structures. Probably, the metallic active sites in Co1 structure are more dispersed than in the just calcined Co2 sample.

Nickel containing samples were also investigated in gas purification field. Preparations of catalyst are described in experimental part. The gasification gas mainly consists of CO, H₂, CO₂, CH₄, H₂O, and N₂, but it also contains impurities, such as tar and ammonia. These impurities must be removed to prevent fouling and blockage of the downstream equipment, as well as NO_x emissions during the gas combustion. Reformed LDH precursors (Figure 24) were used for catalyst preparation for both tar and ammonia decomposition in catalytic hot gas clean-up. Mg/Al hydrotalcite was used and nickel was introduced during the reformation step.

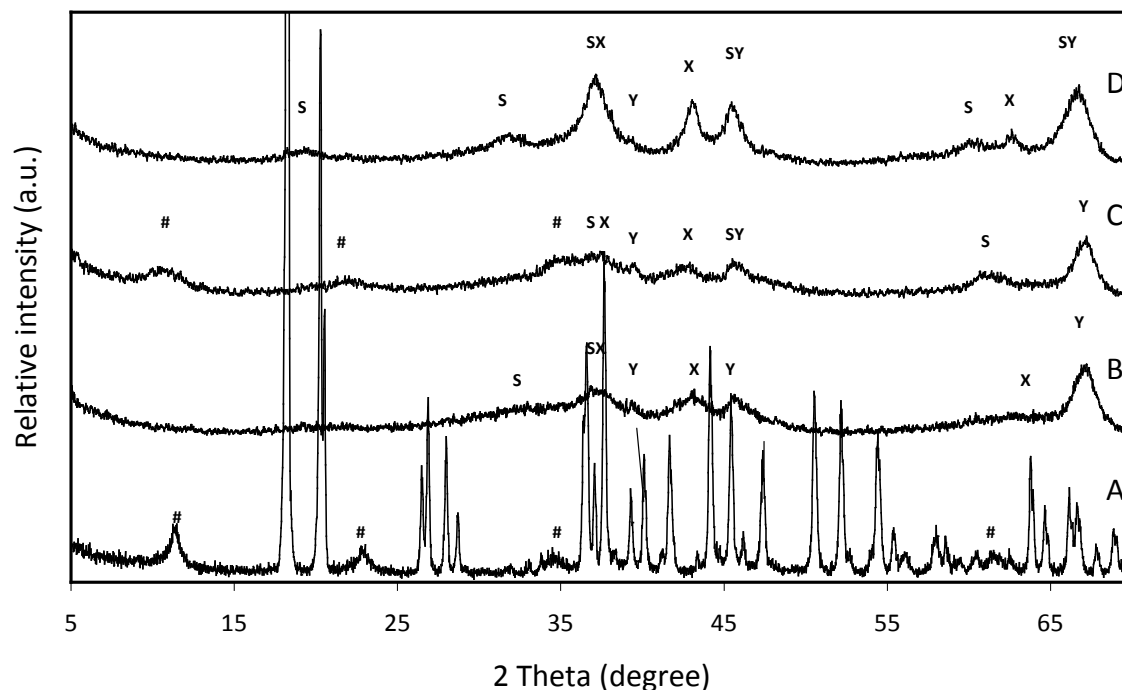


Figure 24. The XRD patterns of: A- hydrotalcite with gibbsite, B- after calcination at 650 °C, C- after Ni addition, and D- Ni1 sample (after final calcination at 850 °C). Crystalline phases: X – MgO, Y - aluminum oxide; S – spinel ;# - hydrotalcite and not market in A diffractogram - gibbsite.

Mg/Al was chosen for two reasons. The as decomposed Mg/Al LDHs can be easier reconstituted to layered structure compared to LDHs containing transition metals. Secondly, these materials were used for the preparation of catalytic blocks due to their cost effectiveness. Two different intermediate calcination temperatures were chosen in order to study the effect of temperature on the final catalyst activity. The lower calcination temperature of 650 °C was selected based on previous reports showing it to be the optimal temperature for the creation of mixed oxide structures [127]. The higher temperature of 850 °C was selected because it is the typical temperature needed for tar decomposition with Ni based catalysts [147]. No fundamental differences between calcination at 650 °C and 850 °C were observed. The conversions of the tar model compound, ammonia and

methane at 700 and 900 °C with and without H₂S in the synthetic gasification gas feed on the non-pre-reduced and reduced catalysts are shown in Table 7. Preparations of catalyst are described in the experimental part.

Table 7. Conversion of the tar model compound, ammonia and methane at 700 and 900 °C without and with H₂S in the feed on nonreduced and reduced catalysts.

| Tar model compound conversion, % | Nonreduced | | | | Reduced | | | |
|-------------------------------------|--------------------------|-----|-----------------------|-----|--------------------------|-----|-----------------------|-----|
| | Without H ₂ S | | With H ₂ S | | Without H ₂ S | | With H ₂ S | |
| Catalyst / T (°C) | 700 | 900 | 700 | 900 | 700 | 900 | 700 | 900 |
| Ni1 | 94 | >95 | 36 | 93 | >95 | >95 | 5 | 93 |
| Ni2 | 74 | >95 | 47 | 92 | >95 | >95 | 28 | >95 |
| Ammonia conversion, | | | | | | | | |
| % | | | | | | | | |
| Catalyst / T (°C) | 700 | 900 | 700 | 900 | 700 | 900 | 700 | 900 |
| Ni1 | 50 | 91 | 15 | 81 | 73 | >95 | 2 | 84 |
| Ni2 | 34 | 89 | 20 | 77 | 81 | >95 | 15 | 92 |
| Methane conversion, % | | | | | | | | |
| Catalyst / T (°C) | 700 | 900 | 700 | 900 | 700 | 900 | 700 | 900 |
| Ni1 | 7 | 40 | 0 | 6 | 76 | 91 | 0 | 9 |
| Ni2 | 16 | 50 | 0 | 3 | 78 | >95 | 9 | 21 |

The obtained data allow us to evaluate the effect of temperature, sulfur content, intermediate calcination temperature and reduction on the conversion ability of the catalyst. As expected, the conversions of the tar model compound, ammonia and methane were higher at 900 °C than at 700 °C for all powdered catalysts. It is indeed well known that the Ni catalyst is active at 900 °C. Without the sulfur addition, the effect of intermediate calcination of the support material depended

on the reaction temperature. At 700 °C, higher conversions of tar and ammonia were observed for Ni1 calcined at lower intermediate temperature. On the other hand, at 900 °C, the intermediate calcination temperature had no discernible effect on the conversions of the tar model compound or ammonia whereas a higher intermediate calcination temperature was favorable for the methane decomposition activity. As expected, the performances of the catalysts were significantly impacted by the presence of sulfur. All catalysts showed higher activities in tar, ammonia and methane decomposition without H₂S than with the feed containing H₂S. The effect of pre-reduction with H₂ was tested by reducing the powder samples prior to activity test (see Table 7). After pre-reduction, the catalyst samples had the same or higher activities towards the tar model compound, ammonia and methane at 900 °C with and without sulfur addition. The positive effect of pre-reduction was observed particularly for methane conversions and without sulfur addition, although at 700 °C only without the addition of sulfur to the gas feed. It might be that the reduced surface offers higher availability of metal nickel compared to the non-reduced catalysts and is also more susceptible to sulfur poisoning which is favored at low temperatures [147]. The reformation of mixed oxides to layered structure and introduction of active cations resulted in the formation of catalyst with promising results for gasification hot gas cleaning.

4. CONCLUSIONS

1. Three layered double hydroxides Mg/Al, Co/Mg/Al and Ni/Mg/Al were successfully synthesized by the low supersaturation method. To our knowledge, for first time, the thermally decomposed and derived mixed metal oxides were reformed to layered structures in water and in magnesium nitrate media.
2. XRD measurements provided direct evidence for phase transformation processes during calcination and reformation of layered structure at different temperatures. From XRF and TG analyses data the formulas of synthesized LDHs $[\text{Mg}_{0.77}\text{Al}_{0.23}(\text{OH})_2](\text{CO}_3)_{0.115} \cdot \text{H}_2\text{O}$, $[\text{Mg}_{0.62}\text{Co}_{0.12}\text{Al}_{0.26}(\text{OH})_2](\text{CO}_3)_{0.13} \cdot 0.91 \text{H}_2\text{O}$ and $[\text{Mg}_{0.65}\text{Ni}_{0.11}\text{Al}_{0.24}(\text{OH})_2](\text{CO}_3)_{0.12} \cdot 1.14 \text{H}_2\text{O}$ were proposed.
3. Incomplete regeneration of Co and Ni containing LDH samples at room temperature in aqueous media has been observed. However, with increasing temperature up to 80 °C the reconstitution process of LDH proceeds fully. The reformation of Co containing LDH in $\text{Mg}(\text{NO}_3)_2$ solution was already observed at room temperature. No essential loss of transition metals during the reformation of mixed metal oxides to LDH was detected. Changes in cationic composition after reformation could be explained by the increase of magnesium content when the reconstitution in magnesium nitrate solution was carried out.
4. Hydration favours the formation of LDHs with higher crystallite size in comparison with the LDH samples reformed in magnesium nitrate medium. In most cases, the crystallite size also increased with increasing the temperature of reconstitution media to 80°C.

5. The SEM imaging revealed that the LDH samples after reformation consist of agglomerated particles (1-3 μm) with sharp edges along with a large number of smaller particles. Reformation medium has a considerable influence on the morphology of mixed metal oxides. Moreover, the effects for nickel or cobalt containing samples were found to be different. Nickel containing mixed oxides derived from samples reformed in water showed a minor decrease of specific surface area, pore dimensions and total pore volume compared to the calcined as synthesized sample. Significant decrease of these values were observed for the samples reformed in magnesium nitrate solution. The LDH samples containing cobalt showed contrary results.
6. Catalysts prepared from LDHs containing cobalt or nickel were tested for the application in gas purification. The reformation effect showed positive impact on cobalt containing catalyst for the removal of NO_x . A catalyst derived from Ni containing LDH showed high activity in tar, ammonia and methane removal with and without the feed containing H_2S at 900 $^\circ\text{C}$.

REFERENCES

- [1] W.T. Reichle, *Solid State Ionics*, 22 (1986) 135-141.
- [2] F. Cavani, F. Trifiro, A. Vaccari, *Catalysis Today*, 11 (1991) 173-301.
- [3] X. Duan, D.G. Evans, *Layered Double Hydroxides*, in: D.M.P. Mingos (Ed.) *Structure and Bonding* (Berlin), Springer-Verlag Berlin Heidelberg, 2006, pp. 242.
- [4] S. Abello, F. Medina, D. Tichit, J. Perez-Ramirez, Y. Cesteros, P. Salagre, J.E. Sueiras, *Chemical Communications*, (2005) 1453-1455.
- [5] H.S. Shin, M.J. Kim, S.Y. Nam, H.C. Moon, *Water Science and Technology*, 34 (1996) 161-168.
- [6] S.J. Palmer, R.L. Frost, *Industrial & Engineering Chemistry Research*, 49 (2010) 8969-8976.
- [7] M.R. Othman, Z. Helwani, M. Martunus, W.J.N. Fernando, *Applied Organometallic Chemistry*, 23 (2009) 335-346.
- [8] Z. Yong, A.E. Rodrigues, *Energy Conversion and Management*, 43 (2002) 1865-1876.
- [9] A.I. Khan, D. O'Hare, *Journal of Materials Chemistry*, 12 (2002) 3191-3198.
- [10] Z.P. Xu, J. Zhang, M.O. Adebajo, H. Zhang, C.H. Zhou, *Applied Clay Science*, 53 (2011) 139-150.
- [11] A. Vaccari, *Catalysis Today*, 41 (1998) 53-71.
- [12] D. Tichit, B. Coq, *CATTECH*, 7 (2003) 206-217.
- [13] A.E. Palomares, A. Uzcategui, A. Corma, *Catalysis Today*, 137 (2008) 261-266.
- [14] A.E. Palomares, J.M. Lopez-Nieto, F.J. Lazaro, A. Lopez, A. Corma, *Applied Catalysis B-Environmental*, 20 (1999) 257-266.
- [15] F. Basile, L. Basini, M.D. Amore, G. Fornasari, A. Guarinoni, D. Matteuzzi, G.D. Piero, F. Trifiro, A. Vaccari, *Journal of Catalysis*, 173 (1998) 247-256.

- [16] M. Marquovich, X. Farriol, F. Medina, D. Montane, *Catalysis Letters*, 85 (2003) 41-48.
- [17] M.S. Li, X.D. Wang, S.R. Li, S.P. Wang, X.B. Ma, *International Journal of Hydrogen Energy*, 35 (2010) 6699-6708.
- [18] K. Schulze, W. Makowski, R. Chyży, R. Dziembaj, G. Geismar, *Applied Clay Science*, 18 (2001) 59-69.
- [19] S.M. Auerbach, K.A. Carrado, P.K. Dutta, *Handbook of Layered Materials*, Marcel Dekker Inc., New York, 2004.
- [20] C.H. Zhou, *Applied Clay Science*, 48 (2010) 1-4.
- [21] A. Vaccari, *Applied Clay Science*, 14 (1999) 161-198.
- [22] G. Centi, S. Perathoner, *Microporous and Mesoporous Materials*, 107 (2008) 3-15.
- [23] D. Tichit, C. Gerardin, R. Durand, B. Coq, *Topics in Catalysis*, 39 (2006) 89-96.
- [24] V. Rives, *Materials Chemistry and Physics*, 75 (2002) 19-25.
- [25] F. Leroux, J.P. Besse, *Chemistry of Materials*, 13 (2001) 3507-3515.
- [26] D.G. Evans, D.A. Xue, *Chemical Communications*, (2006) 485-496.
- [27] V. Rives, M.A. Ulibarri, *Coordination Chemistry Reviews*, 181 (1999) 61-120.
- [28] M. Turco, G. Bagnasco, U. Costantino, F. Marmottini, T. Montanari, G. Ramis, G. Busca, *Journal of Catalysis*, 228 (2004) 43-55.
- [29] E. Angelescu, O.D. Pavel, R. Birjega, M. Florea, R. Zavoianu, *Applied Catalysis a-General*, 341 (2008) 50-57.
- [30] M.A. Aramendia, V. Borau, C. Jimenez, J.M. Marinas, F.J. Romero, F.J. Urbano, *Journal of Materials Chemistry*, 9 (1999) 2291-2292.
- [31] J.D. Phillips, L.J. Vandeperre, *Journal of Nuclear Materials*, In Press, Corrected Proof (2010).
- [32] A. Ayala, G. Fetter, E. Palomares, P. Bosch, *Materials Letters*, 65 (2011) 1663-1665.

- [33] J.S. Valente, J. Hernandez-Cortez, M.S. Cantu, G. Ferrat, E. Lopez-Salinas, *Catalysis Today*, 150 (2010) 340-345.
- [34] M.J. Holgado, F.M. Labajos, M.J.S. Montero, V. Rives, *Materials Research Bulletin*, 38 (2003) 1879-1891.
- [35] N.N. Das, S.C. Srivastava, *Bulletin of Materials Science*, 25 (2002) 283-289.
- [36] B. Zapata, P. Bosch, G. Fetter, M.A. Valenzuela, J. Navarrete, V.H. Lara, *International Journal of Inorganic Materials*, 3 (2001) 23-29.
- [37] J.M. Fernández, C. Barriga, M.A. Ulibarri, F.M. Labajos, V. Rives, *Chemistry of Materials*, 9 (1997) 312-318.
- [38] J. Pérez-Ramírez, J. Overeijnder, F. Kapteijn, J.A. Moulijn, *Applied Catalysis B: Environmental*, 23 (1999) 59-72.
- [39] F.M. Vichi, O.L. Alves, *Journal of Materials Chemistry*, 7 (1997) 1631-1634.
- [40] F. Basile, G. Fornasari, M. Gazzano, A. Vaccari, *Applied Clay Science*, 16 (2000) 185-200.
- [41] P. Benito, I. Guinea, F.M. Labajos, J. Rocha, V. Rives, *Microporous and Mesoporous Materials*, 110 (2008) 292-302.
- [42] S. Velu, D.P. Sabde, N. Shah, S. Sivasanker, *Chemistry of Materials*, 10 (1998) 3451-3458.
- [43] S. Velu, K. Suzuki, M. Okazaki, T. Osaki, S. Tomura, F. Ohashi, *Chemistry of Materials*, 11 (1999) 2163-2172.
- [44] D. Tichit, N. Das, B. Coq, R. Durand, *Chemistry of Materials*, 14 (2002) 1530-1538.
- [45] T. Hibino, A. Tsunashima, *Chemistry of Materials*, 9 (1997) 2082-2089.
- [46] O. Meyer, F. Roessner, R.A. Rakoczy, R.W. Fischer, *Chemcatchem*, 2 (2010) 314-321.
- [47] O. Krasnobaeva, I. Belomestnykh, G. Isagulyants, T. Nosova, T. Elizarova, D. Kondakov, V. Danilov, *Russian Journal of Inorganic Chemistry*, 54 (2009) 495-499.

- [48] S.V. Prasanna, P.V. Kamath, C. Shivakumara, *Materials Research Bulletin*, 42 (2007) 1028-1039.
- [49] E.A. Gardner, S.K. Yun, T.H. Kwon, T.J. Pinnavaia, *Applied Clay Science*, 13 (1998) 479-494.
- [50] R.L. Frost, A.W. Musumeci, T. Bostrom, M.O. Adebajo, M.L. Weier, W. Martens, *Thermochimica Acta*, 429 (2005) 179-187.
- [51] R. Zvoianu, R. Bîrjega, O.D. Pavel, A. Cruceanu, M. Alifanti, *Applied Catalysis A: General*, 286 (2005) 211-220.
- [52] S. Miyata, *Clays and Clay Minerals*, 31 (1983) 305-314.
- [53] D.G. Costa, A.B. Rocha, W.F. Souza, S.S.X. Chiaro, A.A. Leitão, *Applied Clay Science*, 56 (2012) 16-22.
- [54] T. Sato, H. Fujita, T. Endo, M. Shimada, A. Tsunashima, *Reactivity of Solids*, 5 (1988) 219-228.
- [55] F. Prinetto, G. Ghiotti, P. Graffin, D. Tichit, *Microporous and Mesoporous Materials*, 39 (2000) 229-247.
- [56] S. Paredes, G. Fetter, P. Bosch, S. Bulbulian, *Journal of Materials Science*, 41 (2006) 3377-3382.
- [57] M. Jitianu, M. Zaharescu, M. Bălăsoiu, A. Jitianu, *Journal of Sol-Gel Science and Technology*, 26 (2003) 217-221.
- [58] O. Lorret, S. Morandi, F. Prinetto, G. Ghiotti, D. Tichit, R. Durand, B. Coq, *Microporous and Mesoporous Materials*, 103 (2007) 48-56.
- [59] F. Kovanda, D. Kolousek, Z. Cilova, V. Hulinsky, *Applied Clay Science*, 28 (2005) 101-109.
- [60] J.-M. Oh, S.-H. Hwang, J.-H. Choy, *Solid State Ionics*, 151 (2002) 285-291.
- [61] V. Davila, E. Lima, S. Bulbulian, P. Bosch, *Microporous and Mesoporous Materials*, 107 (2008) 240-246.
- [62] F. Basile, P. Benito, P. Del Gallo, G. Fornasari, D. Gary, V. Rosetti, E. Scavetta, D. Tonelli, A. Vaccari, *Chemical Communications*, (2008) 2917-2919.

- [63] F. Basile, P. Benito, G. Fornasari, V. Rosetti, E. Scavetta, D. Tonelli, A. Vaccari, *Applied Catalysis B-Environmental*, 91 (2009) 563-572.
- [64] E. Scavetta, B. Ballarin, M. Gazzano, D. Tonelli, *Electrochimica Acta*, 54 (2009) 1027-1033.
- [65] G. Fetter, F. Hernández, A.M. Maubert, V.H. Lara, P. Bosch, *Journal of Porous Materials*, 4 (1997) 27-30.
- [66] B. Zapata, P. Bosch, M.A. Valenzuela, G. Fetter, S.O. Flores, I.R. Cordova, *Materials Letters*, 57 (2002) 679-683.
- [67] D. Tichit, A. Rolland, F. Prinetto, G. Fetter, M.D. Martinez-Ortiz, M.A. Valenzuela, P. Bosch, *Journal of Materials Chemistry*, 12 (2002) 3832-3838.
- [68] M.J. Climent, A. Corma, S. Iborra, K. Epping, A. Velty, *Journal of Catalysis*, 225 (2004) 316-326.
- [69] S. Mohmel, I. Kurzawski, D. Uecker, D. Muller, W. Gessner, *Crystal Research and Technology*, 37 (2002) 359-369.
- [70] S. Kannan, R.V. Jasra, *Journal of Materials Chemistry*, 10 (2000) 2311-2314.
- [71] N. Iyi, T. Sasaki, *Applied Clay Science*, 42 (2008) 246-251.
- [72] A. Wegrzyn, A. Rafalska-Lasocha, B. Dudek, R. Dziembaj, *Catalysis Today*, 116 (2006) 74-81.
- [73] R.V. Prikhod'ko, M.V. Sychev, I.M. Astrelin, K. Erdmann, A. Mangel', R.A. van Santen, *Russian Journal of Applied Chemistry (Translation of Zhurnal Prikladnoi Khimii)*, 74 (2001) 1621-1626.
- [74] T.S. Stanimirova, G. Kirov, E. Dinolova, *Journal of Materials Science Letters*, 20 (2001) 453-455.
- [75] A.E. Palomares, J.G. Prato, F. Rey, A. Corma, *Journal of Catalysis*, 221 (2004) 62-66.
- [76] K.L. Erickson, T.E. Bostrom, R.L. Frost, *Materials Letters*, 59 (2005) 226-229.
- [77] F. Kooli, V. Rives, M.A. Ulibarri, *Inorganic Chemistry*, 34 (1995) 5114-5121.

- [78] C. Gennequin, R. Cousin, J.F. Lamonier, S. Siffert, A. Aboukais, *Catalysis Communications*, 9 (2008) 1639-1643.
- [79] T. Stanimirova, T. Stoilkova, G. Kirov, *Geolchemistry, Mineralogy and Petrology*, 45 (2007) 119-127.
- [80] K. Takehira, *Journal of Natural Gas Chemistry*, 18 (2009) 237-259.
- [81] M. Mokhtar, A. Inayat, J. Ofili, W. Schwieger, *Applied Clay Science*, 50 (2010) 176-181.
- [82] J. Rocha, M. del Arco, V. Rives, M.A. Ulibarri, *Journal of Materials Chemistry*, 9 (1999) 2499-2503.
- [83] J.A. van Bokhoven, J.C.A.A. Roelofs, K.P. de Jong, D.C. Koningsberger, *Chemistry-a European Journal*, 7 (2001) 1258-1265.
- [84] P. Benito, I. Guinea, F.M. Labajos, V. Rives, *Journal of Solid State Chemistry*, 181 (2008) 987-996.
- [85] F. Millange, R.I. Walton, D. O'Hare, *Journal of Materials Chemistry*, 10 (2000) 1713-1720.
- [86] T. Hibino, A. Tsunashima, *Chemistry of Materials*, 10 (1998) 4055-4061.
- [87] S.K. Jana, Y. Kubota, T. Tatsumi, *Journal of Catalysis*, 247 (2007) 214-222.
- [88] F. Winter, X. Xia, B.P.C. Hereijgers, J.H. Bitter, A.J. van Dillen, M. Muhler, K.P. de Jong, *The Journal of Physical Chemistry B*, 110 (2006) 9211-9218.
- [89] L.P. Cardoso, J.B. Valim, *Journal of Physics and Chemistry of Solids*, 67 (2006) 987-993.
- [90] J.S. Valente, F. Tzompantzi, J. Prince, J.G.H. Cortez, R. Gomez, *Applied Catalysis B: Environmental*, 90 (2009) 330-338.
- [91] H. Nakayama, N. Wada, M. Tshako, *International Journal of Pharmaceutics*, 269 (2004) 469-478.
- [92] K. Ebitani, K. Motokura, K. Mori, T. Mizugaki, K. Kaneda, *Journal of Organic Chemistry*, 71 (2006) 5440-5447.
- [93] J.J. Alcaraz, B.J. Arena, R.D. Gillespie, J.S. Holmgren, *Catalysis Today*, 43 (1998) 89-99.

- [94] J.I. Di Cosimo, V.K. Diez, M. Xu, E. Iglesia, C.R. Apesteguia, *Journal of Catalysis*, 178 (1998) 499-510.
- [95] H. Schaper, J.J. Berg-Slot, W.H.J. Stork, *Applied Catalysis*, 54 (1989) 79-90.
- [96] S. Velu, C.S. Swamy, *Applied Catalysis A: General*, 119 (1994) 241-252.
- [97] V. Vagvolgyi, S.J. Palmer, J. Kristóf, R.L. Frost, E. Horvıth, *Journal of Colloid and Interface Science*, 318 (2008) 302-308.
- [98] M. Bellotto, B. Rebours, O. Clause, J. Lynch, D. Bazin, E. Elkaim, *Journal of Physical Chemistry*, 100 (1996) 8535-8542.
- [99] J. Perez-Ramirez, S. Abello, N.M. van der Pers, *Chemistry-a European Journal*, 13 (2007) 870-878.
- [100] S. Abello, J. Perez-Ramirez, *Microporous and Mesoporous Materials*, 96 (2006) 102-108.
- [101] S.J. Palmer, A. Soisonard, R.L. Frost, *Journal of Colloid and Interface Science*, 329 (2009) 404-409.
- [102] G. Camino, A. Maffezzoli, M. Braglia, M. De Lazzaro, M. Zammarano, *Polymer Degradation and Stability*, 74 (2001) 457-464.
- [103] H. Tamura, J. Chiba, M. Ito, T. Takeda, S. Kikkawa, *Solid State Ionics*, 172 (2004) 607-609.
- [104] H. Tamura, J. Chiba, M. Ito, T. Takeda, S. Kikkawa, Y. Mawatari, M. Tabata, *Journal of Colloid and Interface Science*, 300 (2006) 648-654.
- [105] J.L. Soares, G.L. Casarin, H.J. Jose, R.D.F.P.M. Moreira, A.E. Rodrigues, *Adsorption*, 11 (2005) 237-241.
- [106] T. Wook Kim, M. Sahimi, T.T. Tsotsis, *Chemical Engineering Science*, 64 (2009) 1585-1590.
- [107] S. Miyata, M. Kuroda, United States patent US 4,299,759, (1981).
- [108] D.P. Debecker, E.M. Gaigneaux, G. Busca, *Chemistry-a European Journal*, 15 (2009) 3920-3935.
- [109] F. Winter, V. Koot, A.J. van Dillen, J.W. Geus, K.P. de Jong, *Journal of Catalysis*, 236 (2005) 91-100.

- [110] S. Kannan, C.S. Swamy, *Catalysis Today*, 53 (1999) 725-737.
- [111] M. Herrero, P. Benito, F.M. Labajos, V. Rives, *Journal of Solid State Chemistry*, 180 (2007) 873-884.
- [112] J.T. Klopogge, R.L. Frost, *Applied Catalysis A: General*, 184 (1999) 61-71.
- [113] J. Perez-Ramirez, G. Mul, F. Kapteijn, J.A. Moulijn, *Journal of Materials Chemistry*, 11 (2001) 821-830.
- [114] Z.P. Xu, H.C. Zeng, *Chemistry of Materials*, 12 (2000) 3459-3465.
- [115] S. Ribet, D. Tichit, B. Coq, B. Ducourant, F. Morato, *Journal of Solid State Chemistry*, 142 (1999) 382-392.
- [116] B. Coq, D. Tichit, S. Ribet, *Journal of Catalysis*, 189 (2000) 117-128.
- [117] L. Chmielarz, P. Kustrowski, A. Rafalska-Lasocha, R. Dziembaj, *Thermochimica Acta*, 395 (2003) 225-236.
- [118] B.R. Venugopal, C. Shivakumara, M. Rajamathi, *Solid State Sciences*, 9 (2007) 287-294.
- [119] J. Perez-Ramirez, G. Mul, F. Kapteijn, J.A. Moulijn, *Materials Research Bulletin*, 36 (2001) 1767-1775.
- [120] G. Mitran, T. Cacciaguerra, S. Loidant, D. Tichit, I.C. Marcu, *Applied Catalysis A: General*, 417-418 (2012) 153-162.
- [121] R. Guil-Lopez, J.A. Botas, J.L.G. Fierro, D.P. Serrano, *Applied Catalysis A: General*, 396 (2011) 40-51.
- [122] A.A. Khassin, T.M. Yurieva, G.N. Kustova, I.S. Itenberg, M.P. Demeshkina, T.A. Krieger, L.M. Plyasova, G.K. Chermashentseva, V.N. Parmon, *Journal of Molecular Catalysis A: Chemical*, 168 (2001) 193-207.
- [123] M. Blanchard, H. Derule, P. Canesson, *Catalysis Letters*, 2 (1989) 319-322.
- [124] F. Li, Q. Tan, D.G. Evans, X. Duan, *Catalysis Letters*, 99 (2005) 151-156.
- [125] G. Fornasari, R. Glockler, M. Livi, A. Vaccari, *Applied Clay Science*, 29 (2005) 258-266.
- [126] M.P. Harold, *Current Opinion in Chemical Engineering*, 1 (2012) 303-311.

- [127] O. Clause, B. Rebours, E. Merlen, F. Trifiro, A. Vaccari, *Journal of Catalysis*, 133 (1992) 231-246.
- [128] P. Benito, F.M. Labajos, V. Rives, *Journal of Solid State Chemistry*, 179 (2006) 3784-3797.
- [129] F. Basile, P. Benito, G. Fornasari, D. Gazzoli, I. Pettiti, V. Rosetti, A. Vaccari, *Catalysis Today*, 142 (2009) 78-84.
- [130] J. Perez-Ramirez, S. Abello, N.M. van der Pers, *Journal of Physical Chemistry C*, 111 (2007) 3642-3650.
- [131] L.J.I. Coleman, W. Epling, R.R. Hudgins, E. Croiset, *Applied Catalysis A: General*, 363 (2009) 52-63.
- [132] C. Resini, T. Montanari, L. Barattini, G. Ramis, G. Busca, S. Presto, P. Riani, R. Marazza, M. Sisani, F. Marmottini, U. Costantino, *Applied Catalysis a-General*, 355 (2009) 83-93.
- [133] K. Takehira, T. Shishido, P. Wang, T. Kosaka, K. Takaki, *Physical Chemistry Chemical Physics*, 5 (2003) 3801-3810.
- [134] A.J. Vizcaíno, P. Arena, G. Baronetti, A. Carrero, J.A. Calles, M.A. Laborde, N. Amadeo, *International Journal of Hydrogen Energy*, 33 (2008) 3489-3492.
- [135] X. Zhai, S. Ding, Z. Liu, Y. Jin, Y. Cheng, *International Journal of Hydrogen Energy*, 36 (2011) 482-489.
- [136] D. Tichit, B. Coq, S. Ribet, R. Durand, F. Medina, *Studies in Surface Science and Catalysis*, Volume 130 (2000) 503-508.
- [137] Y. Cesteros, P. Salagre, F. Medina, J.E. Sueiras, D. Tichit, B. Coq, *Applied Catalysis B-Environmental*, 32 (2001) 25-35.
- [138] K. Jiratova, P. Cuba, F. Kovanda, L. Hilaire, V. Pitchon, *Catalysis Today*, 76 (2002) 43-53.
- [139] F. Kovanda, K. Jiráto^{va}, *Applied Clay Science*, 53 (2011) 305-316.
- [140] C.B. Xu, J. Donald, E. Byambajav, Y. Ohtsuka, *Fuel*, 89 (2010) 1784-1795.

- [141] S. Brunauer, P.H. Emmett, E. Teller, *Journal of the American Chemical Society*, 60 (1938) 309-319.
- [142] E.P. Barrett, L.G. Joyner, P.P. Halenda, *Journal of the American Chemical Society*, 73 (1951) 373-380.
- [143] M.C. Gastuche, G. Brown, M.M. Mortland, *Clay Minerals*, 7 (1967) 177-192.
- [144] O.D. Pavel, R. Zavoianu, R. Bîrjega, E. Angelescu, *Catalysis Communications*, 12 (2011) 845-850.
- [145] H.W. Olf, L.O. Torres-Dorante, R. Eckelt, H. Kosslick, *Applied Clay Science*, 43 (2009) 459-464.
- [146] W.T. Reichle, S.Y. Kang, D.S. Everhardt, *Journal of Catalysis*, 101 (1986).
- [147] J. Hepola, Sulfur transformations in catalytic hot gas cleaning of gasification gas, in: VTT, 2000.

LIST OF PUBLICATIONS

Journal articles

- [1] K. Klemkaite, I. Prosycevas, R. Taraskevicius, A. Khinsky, A. Kareiva, Synthesis and characterization of layered double hydroxides with different cations (Mg, Co, Ni, Al), decomposition and reformation of mixed metal oxides to layered structures, *Central European Journal of Chemistry*, 9 (2011) 275-282.
- [2] K. Klemkaite, A. Khinsky, A. Kareiva, Reconstitution effect of Mg/Ni/Al layered double hydroxide, *Materials Letters*, 65 (2011) 388-391.
- [3] H. Rönkkönen, K. Klemkaitė, A. Khinsky, A. Baltušnikas, P. Simell, M. Reinikainen, O. Krause, M. Niemelä, Thermal plasma-sprayed nickel catalysts in the clean-up of biomass gasification gas, *Fuel*, 90 (2011) 1076-1089.
- [4] M. Ivanov, K. Klemkaitė, A. Khinsky, A. Kareiva, J. Banys, Dielectric and conductive properties of hydrotalcite, *Ferroelectrics*, 417 (2011) 136-142.

Conference theses

- [1] K. Klemkaite, A. Khinsky, A. Zilinskas, A. Kareiva, Synthesis peculiarities and characterization of Mo-containing Mg/Al layered double hydroxide. 7th International Conference on Inorganic Materials, Biarritz, France 12 - 14 September 2010 p. P1.126.
- [2] M. Ivanov, K. Klemkaite, A. Khinsky, A. Kareiva, J. Banys, Dielectric and conductive properties of hydrotalcite. I Lithuanian-Ukrainian-Polish Meeting on Ferroelectrics Physics LUP I, Vilnius, Lithuania 13-16 September 2010 p. 100.
- [3] K. Klemkaitė, I. Prosyčėvas, K. Khinsky, A. Kareiva, Incomplete Reconstruction of Layered Double Hydroxide with Transition Metals (Ni, Co).

The 12-th International Conference-School Advanced Materials and Technologies, Palanga, Lithuania 27 – 31 August 2010 p. 82.

[4] K. Klemkaitė, A. Khinsky, A. Kareiva, Reconstitution effect of layered double hydroxide containing different cations. FMNT Functional materials and nanotechnologies, Ryga, Latvia 16-19 March 2010 p. 100.

[5] K. Klemkaitė, A. Kareiva, A. Khinsky, Synthesized and reconstituted LDH containing different cations. Chemija 2009, Vilnius, Lithuania 16 October 2009 p. 35.

[6] K. Klemkaitė, A. Khinsky, A. Kareiva, Memory effect in Co/Mg/Al nanosized hydrotalcites. MOLMAT2008, International Symposium on Molecular Materials Toulouse, France 8 - 11 July 2008 p. 85.

CURRICULUM VITAE

Kristina Klemkaitė-Ramanauskė

Date of birth: May 4, 1983.

Place of birth: Vilnius, Lithuania.

E-mail: kristina.klemkaite@chf.stud.vu.lt

Education:

From October 2007 – PhD student at Vilnius University.

2007 – Vilnius University, MSc, Chemistry.

2005 – Vilnius University, BSc, Chemistry.

2001 – Vilnius Užupis Gymnasium, secondary education.

Working experience:

From August 2005 – Nortra Ltd.

SUMMARY IN LITHUANIAN (SANTRAUKA)

Trijų sudėčių sluoksniuoti dvigubi hidroksidai (SDH) Mg/Al, Co/Mg/Al ir Ni/Mg/Al susintetinti bendro nusodinimo esant mažoms koncentracijoms metodu. Šie SDH buvo termiškai suskaidyti, ir gautieji mišrūs metalų oksidai reformuoti vandenyje ir pirmą kartą magnio nitrato tirpale. Naudojant XRF ir TG duomenis nustatytos susintetintų bendro nusodinimo metodu SDH formulės: $[Mg_{0,77}Al_{0,23}(OH)_2](CO_3)_{0,115} H_2O$, $[Mg_{0,62}Co_{0,12}Al_{0,26}(OH)_2](CO_3)_{0,13} 0,91H_2O$ ir $[Mg_{0,65}Ni_{0,11}Al_{0,24}(OH)_2](CO_3)_{0,12} 1,14H_2O$. XRD analizės rezultatai parodė, kad SDH ir mišrių metalų oksidų faziniai kitimai reformavimo metu priklauso nuo proceso temperatūros ir terpės prigimties. Co ir Ni turinčių SDH mėginių sluoksninės struktūros atstatymas kambario temperatūros vandenyje vyksta nepilnai, tačiau pakėlus temperatūrą iki 80 °C pašalinės oksidų fazės reformuotuose pavyzdžiuose nebelieka. Kai SDH atstatymui buvo naudojamas magnio nitrato tirpalas, katijonų sudėtis pakito dėl padidėjusio sluoksninėje struktūroje magnio kiekio, o pereinamieji metalai išlieka SDH sudėtyje. Ryškus temperatūros ir vandeninės terpės poveikis stebimas ne tik reformavimui, bet ir gautų SDH kristalitų dydžiams. Reformuotų vandenyje kristalitų dydžiai didesni nei SDH, gautų naudojant magnio nitrato tirpalą. Be to, SDH kristalitų dydis dažniausiai padidėja pakėlus proceso temperatūrą iki 80 °C. SEM tyrimai parodė, kad reformuoti SDH susideda iš smulkių kristalitų, linkusių sudaryti didesnius aglomeratus. Iškaitinus SDH gautų oksidų morfologija priklauso nuo jų sudėtyje esančio pereinamojo metalo ir reformavimui naudoto tirpalo prigimties. Mišrūs oksidai su nikeliu, gauti suskaidžius SDH reformuotus vandenyje, pasižymi nežymiai mažesniu savituoju paviršiaus plotu ir akučių tūriu, nei termiškai paveiktų nereformuotų SDH. Priešingi rezultatai stebėti oksidams, turintiems savo sudėtyje kobaltą. Praktiniai panaudojimai reformuotų SDH tirti NO_x pašalinimo reakcijose ir gazifikacijos metu gaunamų dujų valyme. Kobaltą turinčių SDH mėginių aktyvumas parodė, kad oksidai, gauti iškaitinus SDH, yra perspektyvūs

deNO_x katalizatoriais ir aktyvumas jau stebimas pakankamai žemoje temperatūroje (150 °C). Katalizatoriai, gauti iš nikelį turinčių SDH, 900 °C temperatūroje gali būti sėkmingai naudojami šalinant dervas, amoniaką ir metaną, net įvedus H₂S.